MECHANICAL AND RADIATION SHIELDING PROPERTIES OF BORON NITRIDE REINFORCED HIGH-DENSITY POLYETHYLENE

By

KOREY HERRMAN

Bachelor of Science in Chemical Engineering

University of Arkansas

Fayetteville, AR

2017

Submitted to the Faculty of the
Graduate College of the
Oklahoma State University
in partial fulfillment of
the requirements for
the Degree of
MASTER OF SCIENCE
July, 2020

MECHANICAL AND RADIATION SHIELDING

PROPERTIES OF BORON NITRIDE REINFORCED

HIGH-DENSITY POLYETHYLENE

Thesis Approved:

Dr. Ranji Vaidyanathan

Thesis Adviser

Dr. Eric Benton

Dr. Raman P. Singh

ACKNOWLEDGEMENTS

I would like to express my deep and sincere gratitude to my research advisor, Dr. Ranji Vaidyanathan, for giving me the opportunity to do research and providing invaluable guidance throughout this research. He taught me a great deal about conducting research, as well as providing opportunities to grow further through conferences and internships. I am extremely grateful for all he has done for me during my time at Oklahoma State University – Tulsa. I would also like to thank Dr. Eric Benton for his guidance throughout my research as well. He helped in conducting radiation experiments that wouldn't have been possible otherwise. I would also like to thank him for his financial support during the final year of my graduate program.

I would like to thank Dr. Raman Singh for allowing the use of his laboratory. He provided the AFM and Brabender Mixer that were used throughout this experiment. I would like to thank Dr. Kunal Mishra for helping in conducting the AFM experiments and providing help with conference presentations and publishing papers.

I am also grateful to my research lab colleagues, Lynsey Baxter, Dilli Dhakal, and Vishanth Uppu. I appreciate them for their help in conducting the experiments discussed, as well as providing training on equipment that was new to me.

Finally, I would like to thank my parents, Kevin and Roxann Herrman, my sister, Kaisha Shea, and my boyfriend, Matthew Calhoun, for their love, prayers, understanding and continuing support to complete this research.

Name: KOREY HERRMAN

Date of Degree: JULY 2020

Title of Study: MECHANICAL AND RADIATION SHIELDING PROPERTIES OF BORON NITRIDE REINFORCED HIGH-DENSITY POLYETHYLENE

Major Field: MATERIALS SCIENCE AND ENGINEERING

Abstract

In this study, the mechanical and radiation shielding properties of boron nitride (BN) reinforced high-density polyethylene (HDPE) were investigated. Pure polyethylene is considered the best material to use when shielding against galactic cosmic radiation in space; however, it lacks the mechanical properties necessary for structural applications. The effect of adding boron nitride to HDPE was evaluated by determining the mechanical and radiation shielding properties. The mechanical properties were investigated using varying amounts of BN by weight percent in the HDPE. The results for the flexural modulus showed little variation with changing the amount of BN present; however, the compressive modulus and tensile properties showed an increase when using above 5 wt.% BN. The results of these three tests were reinforced by the atomic force microscope (AFM). The storage modulus, loss modulus, and damping factor were found using dynamic mechanical analysis (DMA). The results of DMA showed higher values for storage modulus, loss modulus, and damping factor than for neat HDPE. The combination of these results led to the conclusion that higher amounts of boron nitride lead to better mechanical properties for the composite material. The number of extrusions the filament was exposed to was also considered during this study. This was investigated to determine if heating the sample multiple times would result in a negative effect on the mechanical properties. Performing multiple extrusions on the sample had little to no effect on the storage and loss modulus and resulted in a slight increase of the damping factor. The AFM results proved that by doing multiple extrusions, the BN would form agglomerates in HDPE. Two forms of radiation tests were also performed during this study: neutron exposure and heavy ion exposure. The neutron exposure tests were conducted on varying amounts of BN in the HDPE. For higher amounts of BN in HDPE, the shielding effectiveness increases. For the heavy-ion medical accelerator in Chiba, Japan (HIMAC) tests, a 30 wt.% BN-HDPE composite tank was tested using air and water as fillers. Compared to no shield, the tank proved to shield against the heavy ions when air and water were used as fillers, with water proving to be a better shield.

TABLE OF CONTENTS

Chapter Page

LIST OF TABLES

Table Page

LIST OF FIGURES

CHAPTER I

INTRODUCTION

1.1 Motivation

The desire and drive to send humans into space is a mission that has expanded over decades. Ever since the first U.S. crew program, Mercury back in 1962, the world has had a fascination with sending more humans into space to explore what is around us [1]. A dream was realized in 1969 when Neil Armstrong became the first human to step foot on the moon during the Apollo 11 mission [2]. Sending a human to the moon may seem like a stopping point for the space program, but it was just the beginning. Since then the International Space Station was developed and has been orbiting the Earth since November 1998 and continuously occupied since November 2000 [3].

After the International Space Station (ISS) was considered a success, the drive to return to space became even stronger. This led to the development of Project Constellation in 2003, which was supposed to be the program that took humans to the moon again, and eventually Mars. However, a lack of funding and crucial developments led to the cancellation of this program [4]. Since then researchers have been working to find more cost-effective ways to send humans back to the moon. One way to cut the costs associated with space flight is to investigate the use of new, lighter materials as replacements for parts of the space shuttles, as well as their pay loads.

When designing these lightweight materials, it is important to consider the structural properties, but also ensure the materials provide adequate radiation shielding for the astronauts. During space flight, there are three major forms of radiation exposure: galactic cosmic rays (GCR), solar particle events (SPE), and trapped radiation particles [5]. GCR are particles that come from outside the solar system, but from within the Milky Way galaxy. "GCR is composed of the nuclei of atoms that have had their surrounding electrons stripped away and are traveling at nearly the speed of light" [6]. SPE are particles that are "produced by the acceleration across the transition shock boundary of propagating coronal mass ejecta" [7]. Trapped radiation occurs due to the Earth's magnetosphere. The "trapped" particles consist of protons, electrons, and heavier ions, and are known as the Van Allen belts [8]. These three forms of radiation exposure can be seen in figure 1.

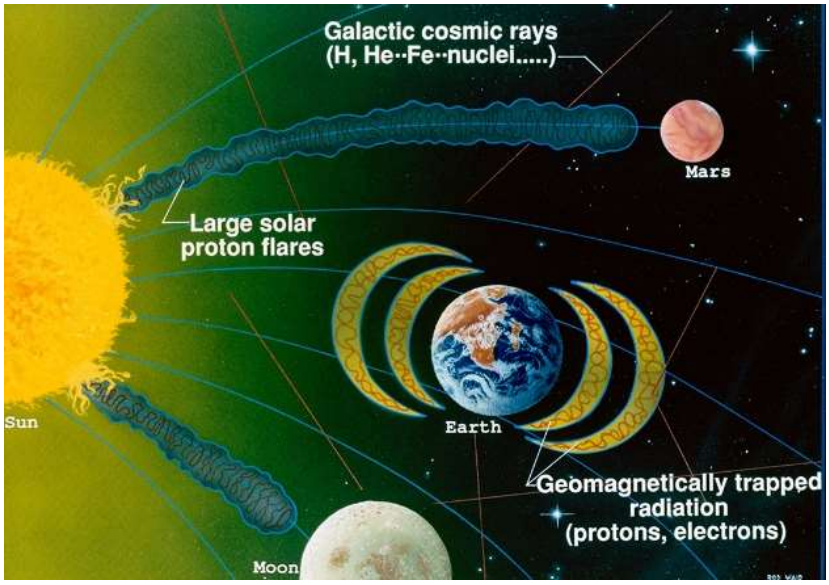

Figure 1: Space Radiation Exposure [9]

1.2 Composites in Space

When considering radiation shielding qualities, hydrogen is the best element to use. “Hydrogen is effective at (1) fragmenting heavy ions such as are found in galactic cosmic radiation (GCR), (2) stopping protons such as are found in solar particle events (SPE), and (3) slowing down neutrons such as are formed as secondaries when the GCR and SPE interact with matter” [5]. However, a shield of hydrogen is impractical. Therefore, current research is looking at materials that are high in hydrogen content, such as polyethylene, CH_2. Polyethylene is 50% better at shielding solar flares and 15% better for cosmic rays, when compared to aluminum, the current material used for space shuttles [10]. However, polyethylene lacks the strength necessary to be a load-bearing aerospace structure.

The next step is finding an additive to use with polyethylene as a base material to create a composite with the appropriate strength and radiation shielding capabilities for space flight. Different research groups have tried a variety of different additives to see which would provide the best results to achieve this goal. Some of the additives that have been considered at this point include graphite, lead oxide, boron carbide, and boron nitride [11] [12] [13] [14].

In this study, boron-based materials were considered as potential additives for the polyethylene. “Boron has one of the largest neutron absorption cross-sections of all the elements of the periodic table” so it provides greater radiation shielding abilities, while also providing strength to the structure [5]. Boron carbide and boron nitride were both considered as additives. “Boron carbide is a material that is well known for its hardness, high level of mechanical strength and melting point beside the low specific

gravity along with the high neutron absorption cross-section of 767 barn in the thermal energy region because of ^{10}B isotope of Boron and makes it valuable material for shielding purposes" [11]. Boron nitride has similar properties to that of boron carbide. Additionally, hexagonal boron nitride (h-BN) is a good choice due to the wear-resistant properties it has from its structure, which is similar to that of graphite [5]. The structure of h-BN can be seen in figure 2.

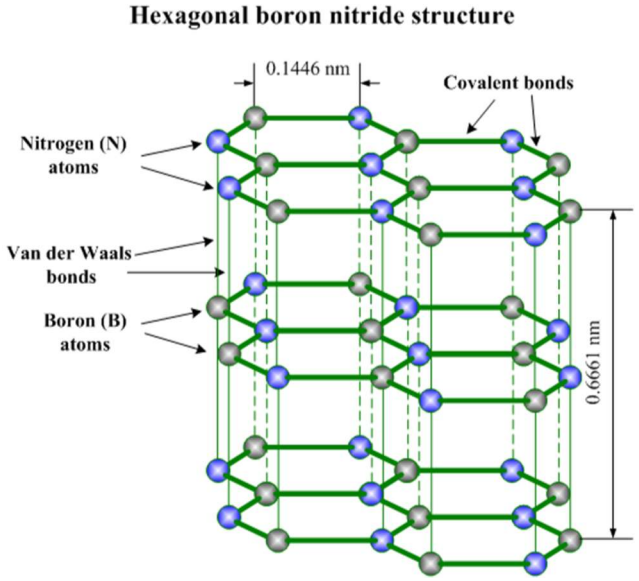

Figure 2: Structure of h-BN

1.3 FLUKA Modeling

Prior to this study, Rajesh Panthi and Eric Benton from the Radiation Physics Laboratory at Oklahoma State University used FLUKA Monte Carlo computer-based simulations of the radiation shielding properties of materials containing boron nitride developed by the Vaidyanathan group [15]. The FLUKA simulations were conducted for both 1 GeV/n energy ^{28}Si and ^{56}Fe ion beams. From these results, the LET spectra, absorbed dose, and equivalent dose were calculated to use as a comparison for the test results obtained from the HIMAC test results performed during the current study.

A schematic diagram for the FLUKA simulation is shown in figure 3 [15]. There are fourteen separate absorbers, each with a depth of 5.0 g/cm^2. The absorbers were assigned with pure polyethylene, polyethylene containing varying amounts of boron nitride, and pure boron nitride. The concentrations of boron nitride considered in this experiment were 10%, 25%, 50%, 75%, and 90% by mass. CR-39 equivalent water filled detectors were placed at incremental depths of 5 g/cm^2 ranging from 0 to 70 g/cm^2. The detectors were 4 cm x 4 cm, which is the same as the cross-sectional size of the ion beams used.

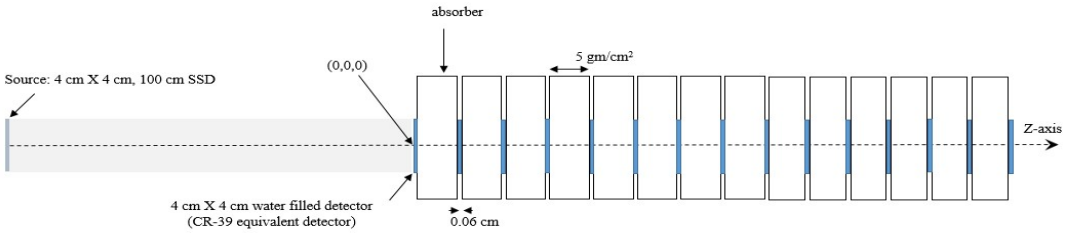

Figure 3: Schematic diagram of geometry used in FLUKA simulations

1.3.1 Si Beam Simulations

The $LET_{\infty}H_2O$ spectra scored by the fifteen detector positions at different depths within various absorbers for simulated exposures to a beam of 1 GeV/n ^{28}Si were obtained [15]. The spectra for pure polyethylene and polyethylene with 10% boron nitride are shown in figure 4 as examples [15]. From these spectra, the absorbed dose was calculated, and then normalized to the absorbed dose at 0 g/cm^2. These results are shown in figure 5.

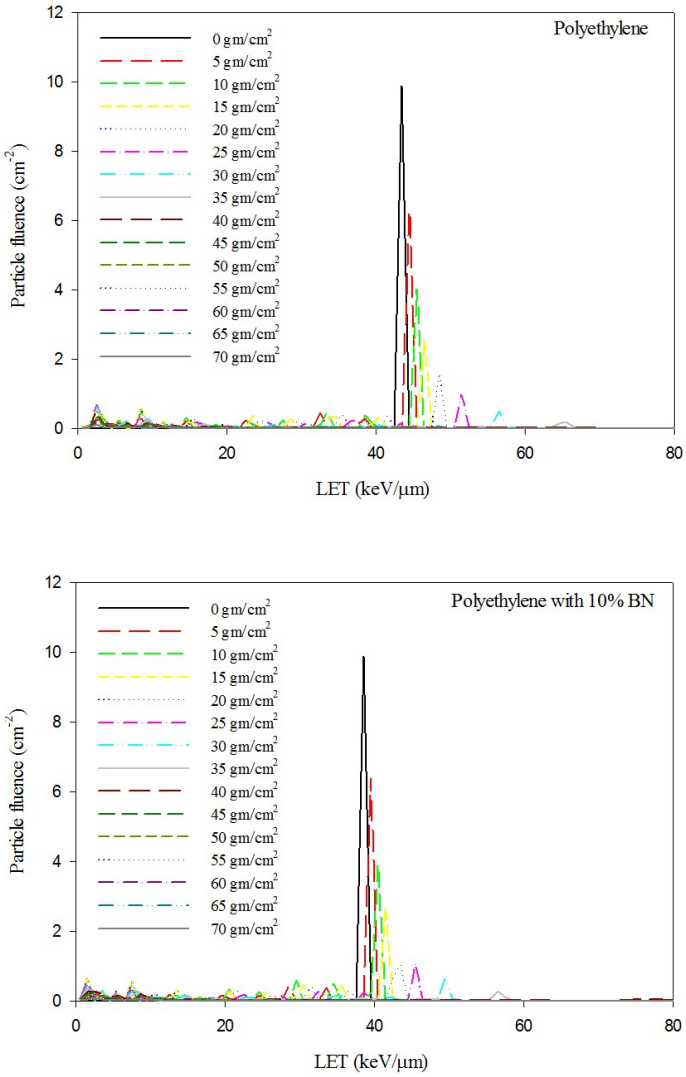

Figure 4: LET Spectra for polyethylene (top) and polyethylene with 10% BN (bottom)

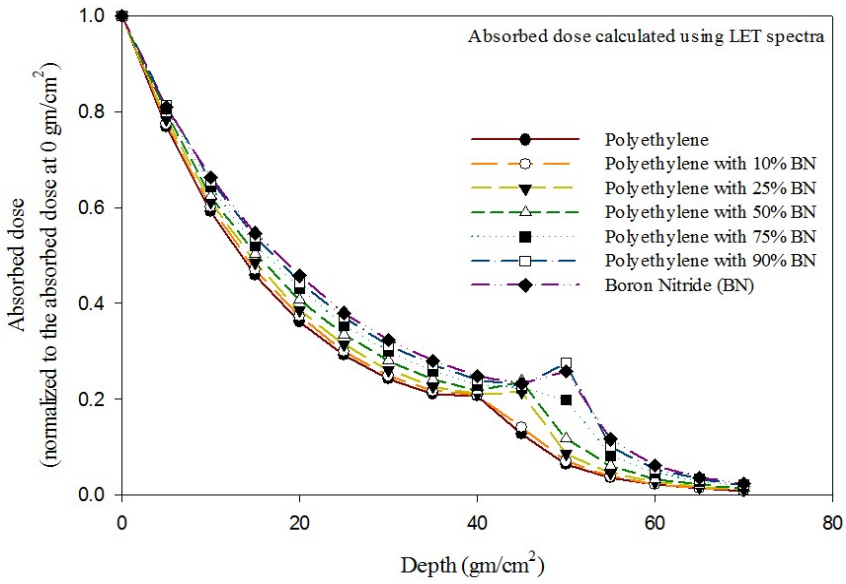

Figure 5: Absorbed dose at different depths for simulated exposures to a beam of 1 GeV/n ^{28}Si

From the absorbed dose, the equivalent dose could also be found. The equivalent dose was also normalized to 0 g/cm^2 for each medium considered in the simulation. These normalized values are plotted in figure 6.

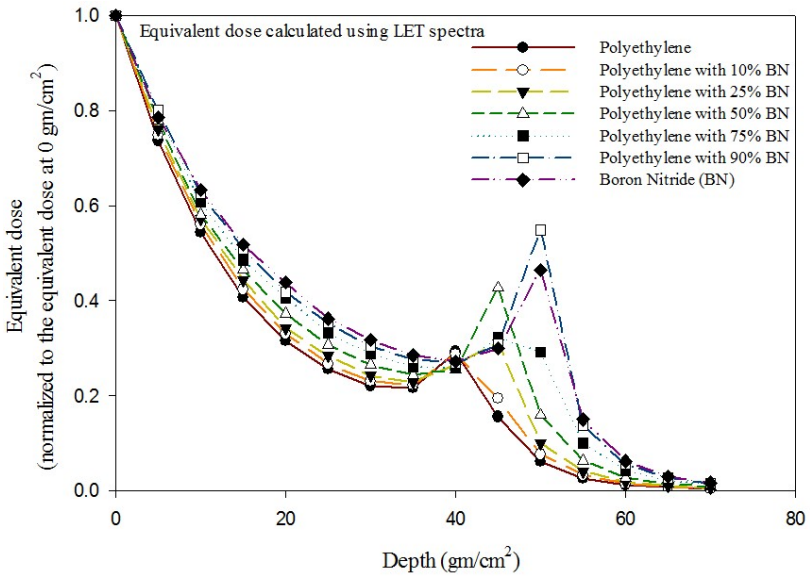

Figure 6: Equivalent dose calculated using LET spectra for simulated exposures to a beam of 1 GeV/n ^{28}Si

When the beams of high Z ions pass through a material such as polyethylene, some part of the beams kinetic energy is transferred into the material at a certain rate which is then given by the linear energy transfer (LET). In the shallow parts of the material, the LET occurs mainly due to the ionization created by the primary ions. The lower Z ions that are created by the fragmentation of the primary ions are called projectile fragments. Since the fragmentation occurs at deeper parts of the material, the projectile fragments have even smaller kinetic energy per nucleon. Each of these projectile fragments creates its own track and transfers part of its kinetic energy into the material at different values.

As shown by the LET spectrum calculated at a depth of 0 g/cm^2, there is only one peak which is known as the primary ionization peak produced by the primary ions. Once the fragmentation occurs, this peak will decrease at the greater depths. Eventually the primary ionization peak will shift towards the higher LET and then beyond the range of the beam no more ionization will occur, and the peaks will disappear completely. However, the fluence of the projectile fragments will increase at these greater depths, and those peaks will be visible. The LET spectra for each material can be used to calculate the percentage of the primary ^{28}Si ions that get fragmented into lower Z ions at different depths. These values can be seen in figure 7.

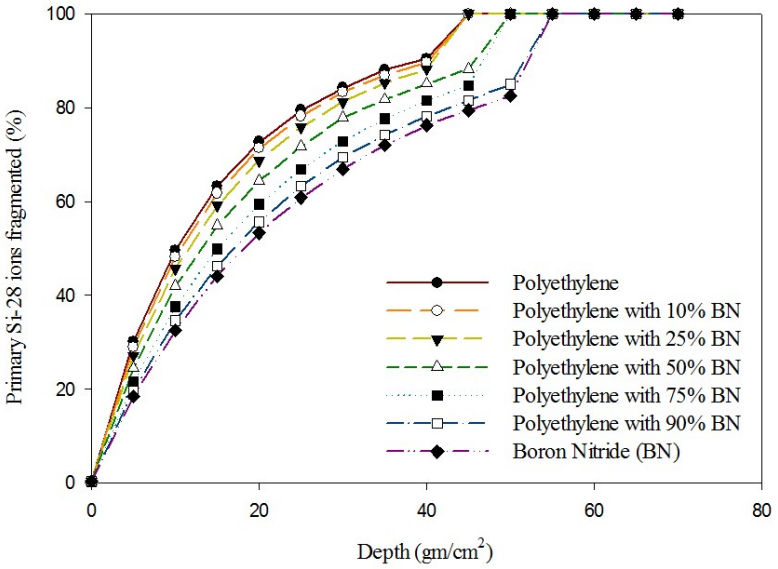

Figure 7: Percent fraction of the primary ions fragmented as a function of depth in various media for simulated exposures to a beam of 1 GeV/n ^{28}Si

1.3.2 Fe Beam Simulations

The process to obtain the $LET_{\infty}H_2O$ spectra for the 1 GeV/n ^{56}Fe was the same as for the ^{28}Si beam. Examples of the LET spectra obtained are shown in figure 8. From this data, the absorbed dose was again calculated and then normalized to 0 g/cm^2. This data is shown in figure 9.

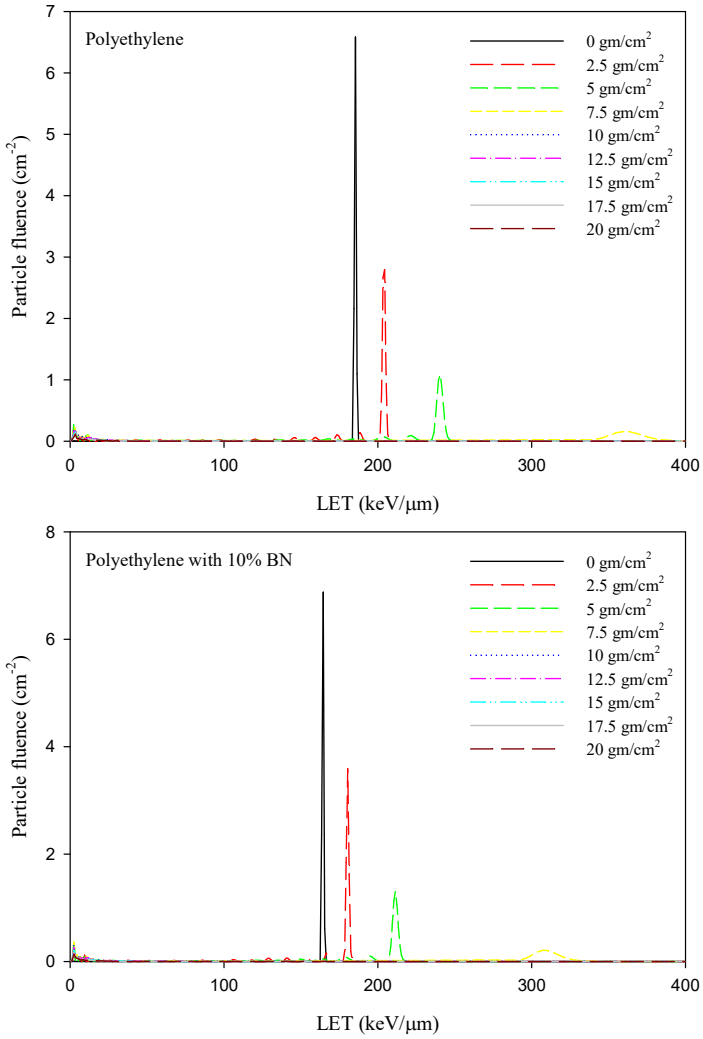

Figure 8: LET spectra for polyethylene (top) and polyethylene with 10% BN (bottom)

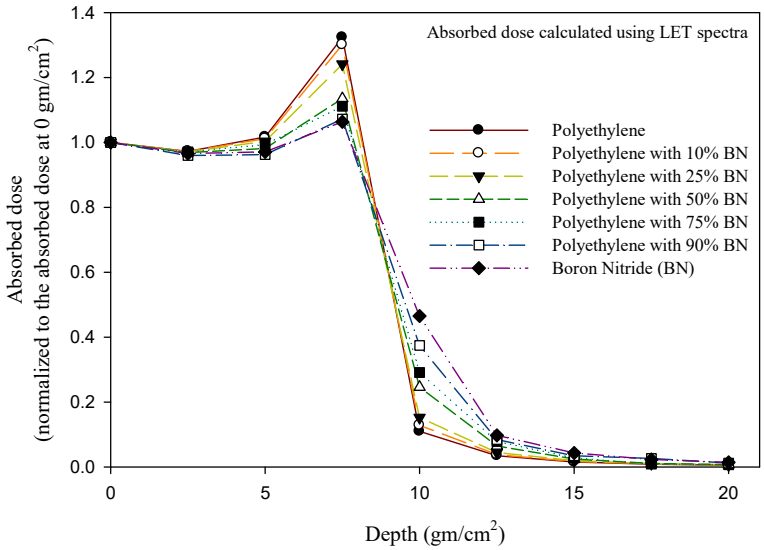

Figure 9: Absorbed dose calculated using LET spectra for simulated exposure to a 1 GeV/n ^{56}Fe beam

Again, the equivalent dose was calculated from the LET spectra and then normalized to 0 g/cm^2. The results for this are shown in figure 10.

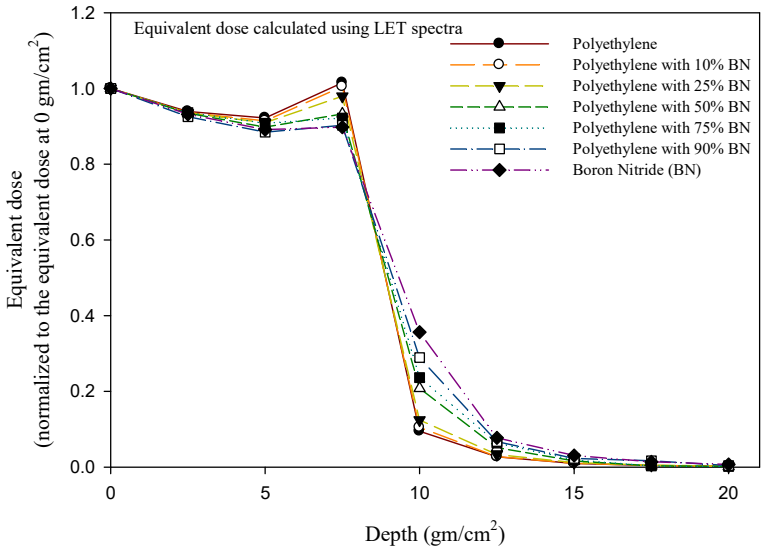

Figure 10: Equivalent dose calculated using LET spectra for simulated exposure to a 1 GeV/n ^{56}Fe beam

Similar to the ^{28}Si beam, the primary ionization peak for the ^{56}Fe beam shifts toward the higher LET with the increase in depth, and beyond the range of the beam

no ionization occurs due to the primary ions and primary ionization peak completely disappearing. Again, however, the fluence of projectile fragments increases with depth, so peaks corresponding to this can be seen. The percentage of the primary ^{56}Fe ions that get fragmented into lower Z ions are different depths was calculated and is shown in figure 11.

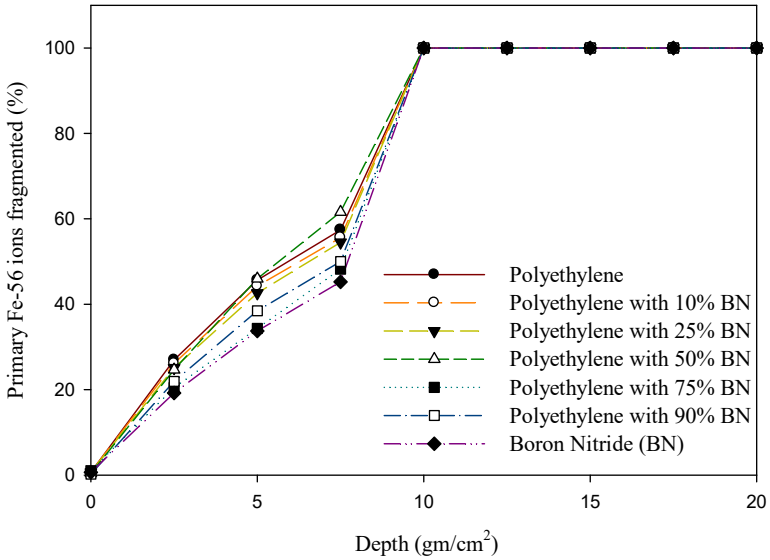

Figure 11: Percent fraction of the primary ions fragmented as a function of depth in various media following simulated exposure to a 1 GeV/n ^{56}Fe beam

1.4 Motivation for the Present Study

Results from the FLUKA simulations indicated that the addition of boron nitride to the polyethylene in varying amounts has little effect on the shielding properties of polyethylene as these beams propagate through shielding targets. Even though this seems like a negative result, it was the basis for the study being presented here. Polyethylene is considered the gold standard for space radiation shielding due to its high concentration of hydrogen, so by determining that the addition of boron nitride doesn't completely hinder the shielding capabilities, it creates an opportunity to use it

for space applications. Thus, if it can be proven that the boron nitride provides sufficient increase in the structural or mechanical properties of the composite, then it could be a contender for structural applications in the aerospace industry. This was the motivation for the present study.

CHAPTER II

METHODOLOGY

2.1 Composite Development

In these experiments, composite materials were created using polyethylene as the matrix and boron nitride powder as an additive. The radiation shielding properties of polyethylene with boron nitride content varying from 1 to 40% by weight were tested. Since boron nitride does not have any adhesive properties, the amount of boron nitride was maintained below 40 weight percent. This was also based on the fact that polyethylene blocks containing higher than 40% by weight boron nitride could not be consolidated into blocks for testing. Therefore, the samples were prepared with boron nitride varying from 1% to 40% boron nitride by weight. The composite samples were created in 50-gram batches using a laboratory-scale batch mixer (Model VD-52 Prep-Center, C.W. Brabender Instruments, Inc., Hackensack, NJ).

After the preparation of the composite material blend, the blend was removed from the mixer and were pressed in a mold (figure 12) to create sample blocks or extruded to create filaments. The sample blocks (76.2 mm x 76.2 mm or 3” x 3”) were created by placing the polyethylene blend in an aluminum mold, heated in an oven by applying a compressive force. The sample blocks (figure 13) were created to perform mechanical testing, as the blocks could be machined to the dimensions specified for each mechanical

tests ASTM standards. The filaments were created by putting the sample pieces directly in a Filabot EX2 Extruder and Spooler system, shown in figure 14. The sample pieces were heated up and then extruded to create a round filament, which was then passed through a set of rollers and wound to create a flat filament as shown in figure 14. The filament preparation process is as follows: the blended material was broken up manually into small pieces and fed into a hopper/screw combination and heated to almost melting point of the feedstock material. Two types of filaments could be produced, based on whether the filament is fed through a set of compressive rollers, which can be engaged or disengaged. Depending on the roller position, the filament could be either a circular one (1.778 mm diameter) or a flat filament, with a maximum of approximately 2 mm width filament for the maximum pressure. It was felt that the filament is flat would provide the most uniform results that could best fit the filament winding process for a composite tank. The flat filaments were used to create the composite tanks for radiation testing. Some filaments were also used to test if multiple extrusions would influence the mechanical properties of the sample. Table 1 and 2 show the processing conditions and the resulting diameter of the filaments of the various PE-BN materials, which is the preferred radiation shielding material to protect against GCR.

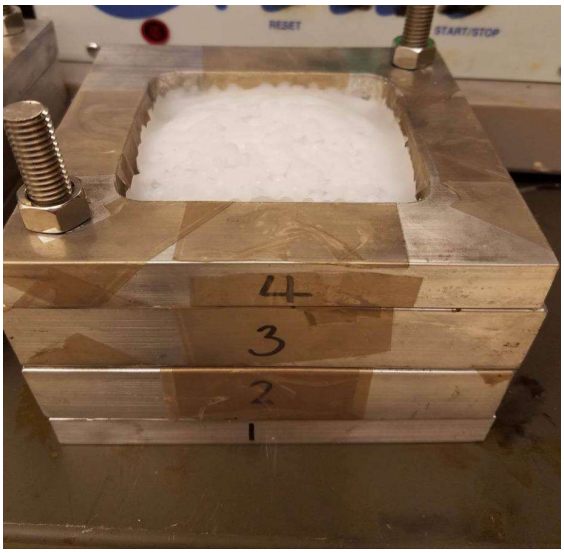

Figure 12: Mold Used for Pressing PE-BN blocks

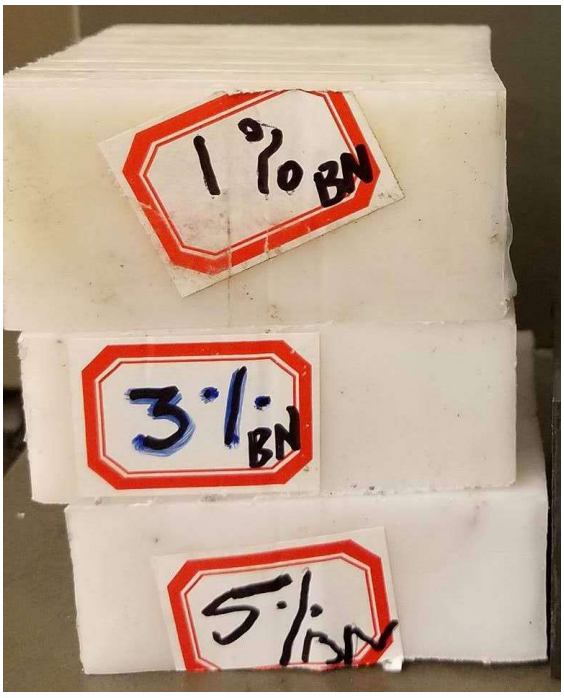

Figure 13: Samples of PE-BN Blocks Prepared with 3 Different BN Contents

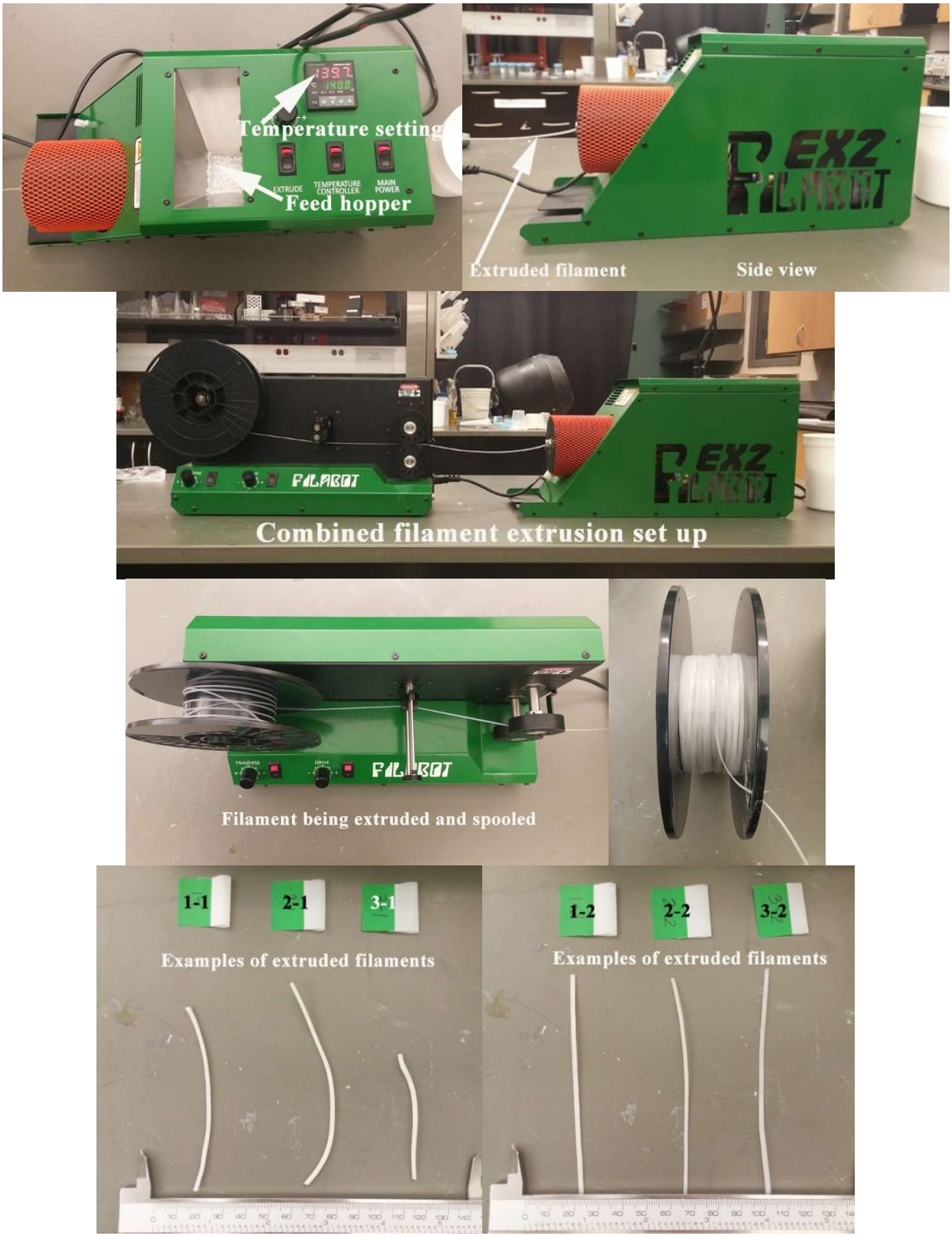

Figure 14: Filabot Extrusion Equipment and the Resulting Filaments (numbers showing filaments match the processing conditions shown in Tables 1 and 2)

Table 1: Processing Condition Description for Filament Extrusion Using Filabot Equipment

Sample	Processing Condition Description
(1-1)	Uncompressed sample heated at 140°C
(1-2)	Compressed sample heated at 140°C
(2-1)	Uncompressed sample heated at 150°C
(2-2)	Compressed sample heated at 150°C
(3-1)	Uncompressed sample heated at 160°C
(3-2)	Compressed sample heated at 160°C
*All samples taken with an extrusion speed of ~9-10 and a drive speed ~2.27 turns Figure 14 shows correct drive speed dial location turned clockwise from the zero position	

Table 2: Filament Dimensions of Extruded Filaments using Processing Conditions in Table 1

Sample Label	Diameter (mm)		Sample Label	Diameter (mm)		Thickness (mm)	
(1-1)	2.14	Average	(1-2)	1.97	Average	1.12	Average
	1.74	1.89		2.04	2.00	1.10	1.12
	1.99	Standard		1.99	Standard	1.10	Standard
	1.83	Deviation		1.97	Deviation	1.16	Deviation
	1.76	0.17		2.02	0.03	1.11	0.69
(2-1)	1.73	Average	(2-2)	1.79	Average	0.73	Average
	1.85	1.98		1.64	1.81	0.69	0.69
	2.05	Standard		1.82	Standard	0.68	Standard
	2.22	Deviation		1.85	Deviation	0.69	Deviation
	2.03	0.19		1.94	0.11	0.67	0.02
(3-1)	1.79	Average	(3-2)	2.05	Average	0.51	Average
	2.04	2.07		2.19	2.09	0.54	0.53
	2.04	Standard		2.29	Standard	0.50	Standard
	2.25	Deviation		2.05	Deviation	0.56	Deviation
	2.25	0.19		1.85	0.17	0.52	0.02

The all-composite tank was fabricated by co-mingling the PE-BN filaments along with carbon fiber/epoxy prepreg. The carbon fiber/epoxy prepreg was used to secure the PE-BN filament in place, along with providing additional strength to the tank. The tank created was approximately 0.8 m in length and 0.3 m in diameter. Figure 15 shows the tank being fabricated on the filament winder. This tank was prepared with the assistance of Infinite Composites Technologies in Tulsa, OK. Figure 16(a) shows the as prepared tank,

with the PE-BN filament being the white filaments, and figure 16(b) shows the finished and cured tank.

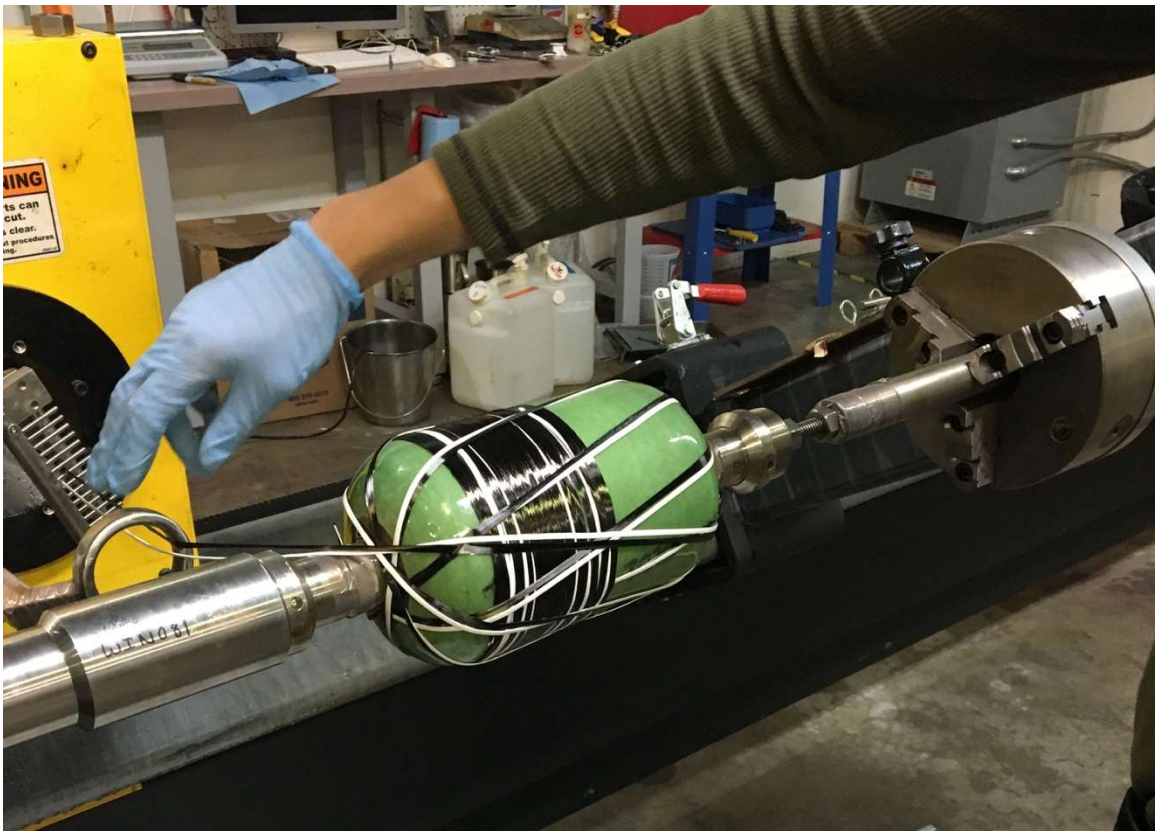

Figure 15: Filament Winding of the Composite Tank for Radiation Shielding Experiments

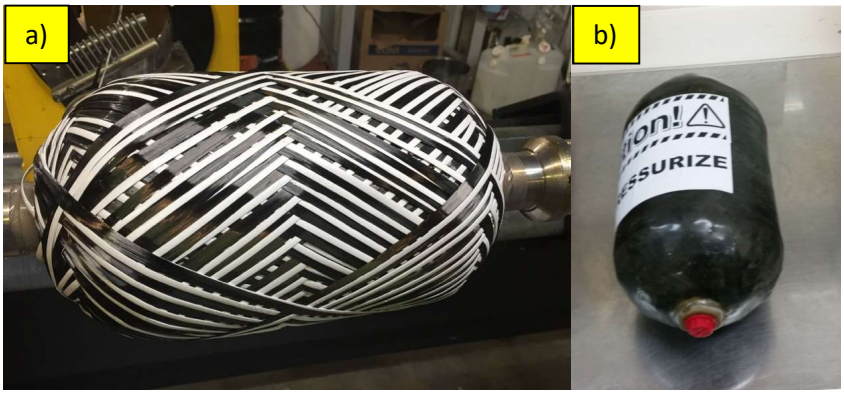

Figure 16: PE-BN Composite Tank. a) fabrication process. b) finished and cured

2.2 Characterization Testing

To narrow down what percentage of boron nitride was necessary for the polyethylene composite, characterization tests were completed. These were used to ensure that the material would have reasonably good strength and stiffness similar to pure polyethylene.

2.2.1 Mechanical Testing

The flexural modulus for samples of PE containing various weight percentages of boron nitride was determined by performing a three-point bend test until failure. These tests were performed following ASTM D790 on the universal testing machine (Instron 5567, Norwood, MA). Samples were machined to be 56 x 12.5 x 3.2 mm from the sample blocks of each composite. Tests were performed in a displacement-controlled mode at a fixed crosshead speed, which was calculated using the following equation.

$$R = ZL^2/6d$$

Where L is the length, d is the thickness, and Z is the rate of straining of the outer fiber. Z shall be equal to 0.01.

The flexural modulus (σ_b) of the sample was determined using the following equation.

$$\sigma_b = \frac{L^3 m}{bd^3}$$

Where L is the span length of the sample, m is the slope calculated from the load-displacement graph, b is the width, and d is the thickness of the sample.

Compressive properties of the samples were obtained using a 30 kN Materials Testing System (Model 5567, Instron, Norwood, MA) using ASTM D695. The tensile modulus and strength were also measured using ASTM D638. These tests were all used to determine the elastic modulus of the samples at various weight percentages of BN, which could be compared to the AFM data.

2.2.2 Atomic Force Microscopy

Atomic force microscopy or AFM (MFP-3D, Asylum Research, Santa Barbara, CA, USA) was used for performing indentions on the PE-BN composite blends. An indenter (AC160TS) with a resonant frequency of 300 kHz and a spring constant of 25 N/m was used for the testing. The experiment was performed using contact mode to create a force map of 48 by 48 grid in a square region of 5 μm.

2.2.3 Dynamic Mechanical Analysis

Dynamic mechanical analysis (DMA) is a technique used to provide information on the mechanical properties of a material, such as storage modulus, loss modulus, and damping factor. Dynamic mechanical analysis of a PE with 30% boron nitride composite was performed using DMA Q800 (TA Instruments, Inc., New Castle, DE). Following ASTM D4065-12, a sample size of 60 x 12.7 x 3.1 mm was cut from a sample block and placed in a dual-cantilever clamp with a span length of 35 mm. Three-point bend tests were carried out while heating the sample from -150°C to 100°C at a ramp rate of 3°C/min and applying a constant sinusoidal displacement of 20 mm with 1 Hz frequency. The three-point bend test provides the storage modulus and the loss modulus. The dampening

coefficient (tan δ) of the sample was measured using a TA instrument's universal analysis software.

2.2.4 Differential Scanning Calorimetry

Differential scanning calorimetry (DSC) is a technique used to obtain the glass transition temperature, or T_g, for a material. The experiments were performed using DSC Q2000 (TA Instruments, Inc., New Castle, DE) under constant flowing nitrogen, with a flow rate of 50 ml/min, following ASTM D3418-15. Approximately 7-8 mg of sample was loaded into the aluminum pans. To study the T_g for the samples, they were first heated to 150°C at a scan rate of 10°C/min, held at that temperature for 5 minutes, and then cooled to 35°C at a rate of 10°C/min. For the second scan, the samples were heated and cooled under the same conditions. The data was taken from the second heating cycle.

2.3 Radiation Testing

2.3.1 Neutron Exposure

Neutron exposure experiments were conducted at the NASA Langley Research Center's Radiation Shielding Materials Lab in Hampton, Virginia. A 1-Curie Americium-Beryllium (AM-BE) neutron source moderated by a polyethylene block was used to conduct the testing, figure 17. The initial neutrons released by the AM-BE source are considered fast neutrons (4.5 MeV) and after passing through the polyethylene block the neutrons become thermal neutrons (< 0.5 MeV). An initial experiment was conducted to develop a basis for the calculations. The basis experiment was performed by using an

Indium foil alone on the source, which was called the “bare foil experiment”. Indium foils are used due to their high neutron absorption cross-section. To run the experiment on the samples, small sample blocks were placed between the neutron source and the foil. The foils will absorb the neutrons that get through the sample block, which is then placed inside the counters to obtain the data. The tests were ran using samples of polyethylene with 1%, 5%, and 30% boron nitride.

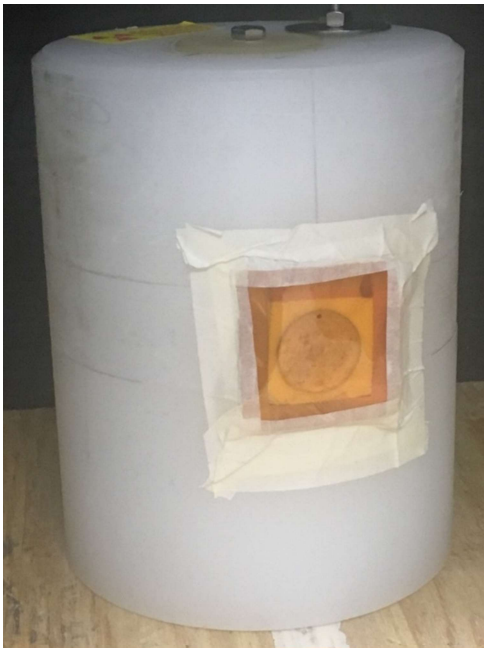

Figure 17: 1-Curie Americium-Beryllium Neutron Source with Polyethylene Block

After the samples are removed from the neutron source, the foil associated with the sample is placed in a Geiger Counter, figure 18, to obtain the absolute radiation, with counts being recorded every 2 minutes. From the Geiger Counter data, the mass absorption cross-section for thermal neutrons, or the shielding effectiveness, can be calculated using the following equation.

$$\mu_m = \frac{-1}{d * t} \ln\left(\frac{A}{A_0}\right)$$

Where μ_m is the mass absorption cross-section for thermal neutrons, t is the sample thickness, d is the sample density, A_0 is the average initial activity of the unshielded foil, and A is the average initial activity of the shielded foil.

Figure 18: Geiger Counter

2.3.2 Heavy Ion Exposure

The radiation shielding properties of all PE-BN composite tank were characterized using heavy ion beams of energy and charged similar to radiation encountered in space. This experiment was conducted using the Heavy Ion Medical Accelerator in Chiba, Japan (HIMAC), figure 19. These experiments were conducted by Dr. Benton's research group. The PE-BN tank was pressurized and exposed to beams of 422 MeV/n ^{56}F and 383 MeV/n ^{16}O. Exposures were made with both the tank containing 1 atm of air and the tank filled with water at 1 atm. The lineal energy spectrum was measured using a tissue equivalent proportional counter (TEPC).

Figure 19: PE-BN Tank Tested Using HIMAC

2.3.3 Materials on the International Space Station Experiments (MISSE)

Samples were prepared and delivered for both the MISSE-9 and MISSE-11 experiments. For MISSE-9, the samples were based on polyethylene blended with boron nitride and boron carbide, while for MISSE-11, samples were based on polyethylene blended with boron nitride and sandwiched with carbon fiber epoxy. For comparison, MISSE-9 also included pure polyethylene, while MISSE-11 also included samples of pure polyethylene, copper and aluminum. MISSE-9 was launched in April 2018 and received back in October 2019. The samples were also included as part of the MISSE-11 experiment, which launched in March 2019 and returned in March 2020. The MISSE-9 experimental samples' dimensions and the samples are shown in figure 20. The sample blocks were 76.2 mm x 76.2 mm x 6.985 mm (3" x 3" x 0.275 thick). In the case of the MISSE-9 samples, the exposed surface area is 63.86 mm x 63.86 mm (2.514" x 2.514"). In the case of the MISSE-11 samples, the PE-BN blocks were sandwiched between 2 carbon fiber/epoxy panels of 3 mm thickness each, shown in figure 21. In the PE-BN

blocks, circular wells were created in the sample to house multiple thermoluminescence detectors (TLDs), as shown in figure 22. The TLDs were used to measure the absorbed dose through the sample block. The sample blocks were secured to the MISSE tray, which was bolted to the MISSE experiment platform at NASA Langley Research Center to be included in the MISSE-9 and MISSE-11 experiments. The sample preparation and the MISSE tray were prepared by Dr. Sheila Thibeault at NASA Langley Research Center.

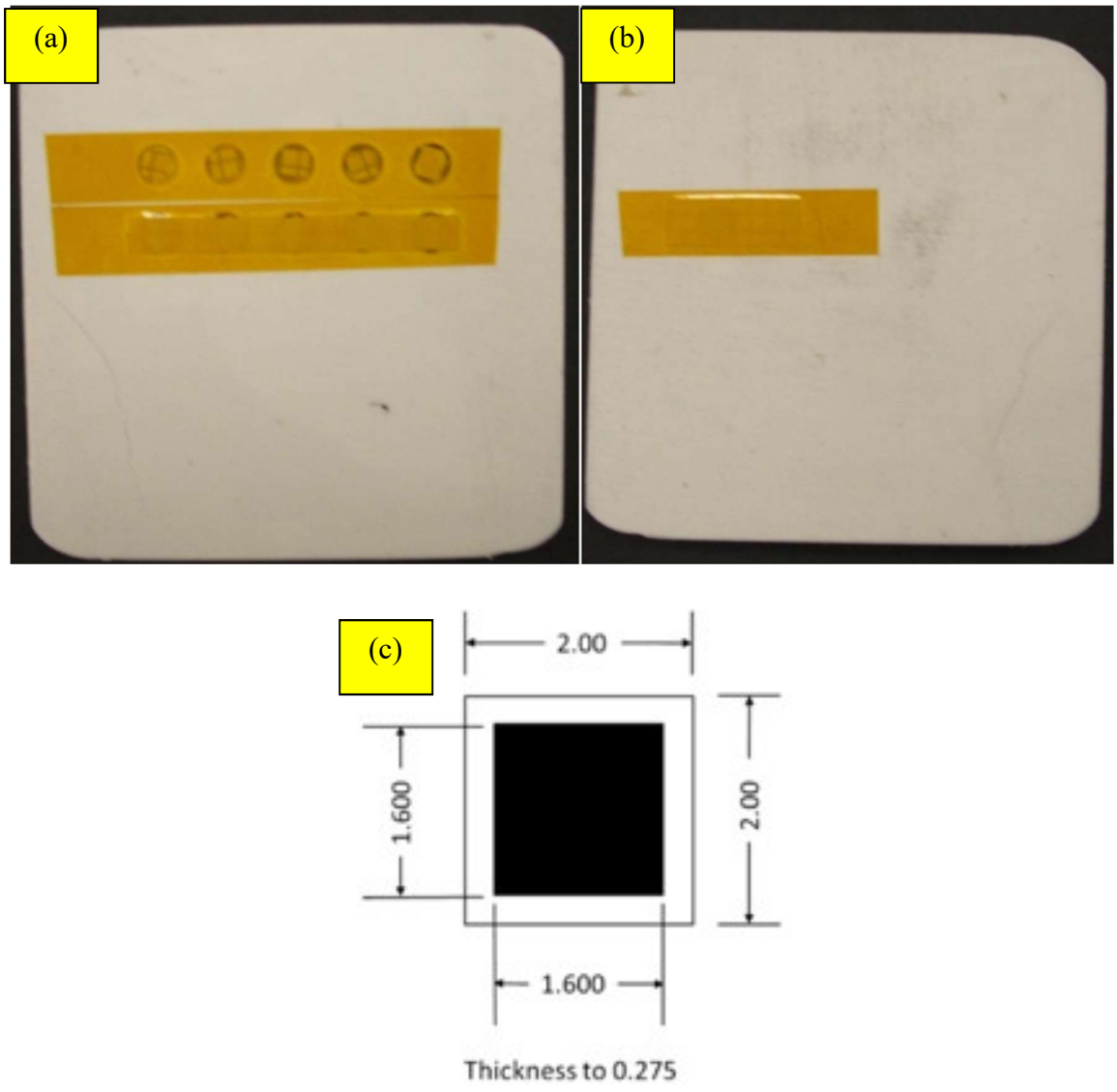

Figure 20: MISSE-9 Samples: (a) PE-BN Sample Facing the MISSE Platform and (b) away from the MISSE Platform, and (c) Sample Dimensions

Figure 21: PE-BN Sandwich Composite for MISSE-11

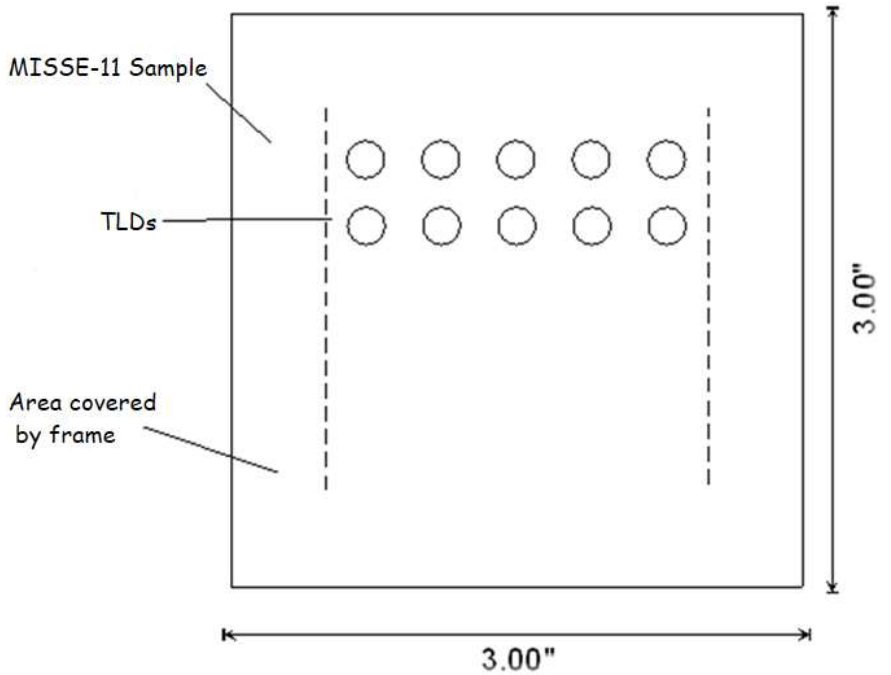

Figure 22: Diagram of PE-BN Sample Block with Detectors for MISSE-11

For both MISSE-9 and MISSE-11, the samples had the same location on the International Space Station. During both experiments, the samples were placed in the Zenith orientation, meaning it was facing away from the Earth, as shown in figure 23(a) [16]. This position has the highest solar exposure and a grazing atomic oxygen (AO) exposure. The location of the PE-BN and PE-BC samples for MISSE-9 can be seen in figure 23(b). For MISSE-11, the samples were in the same location.

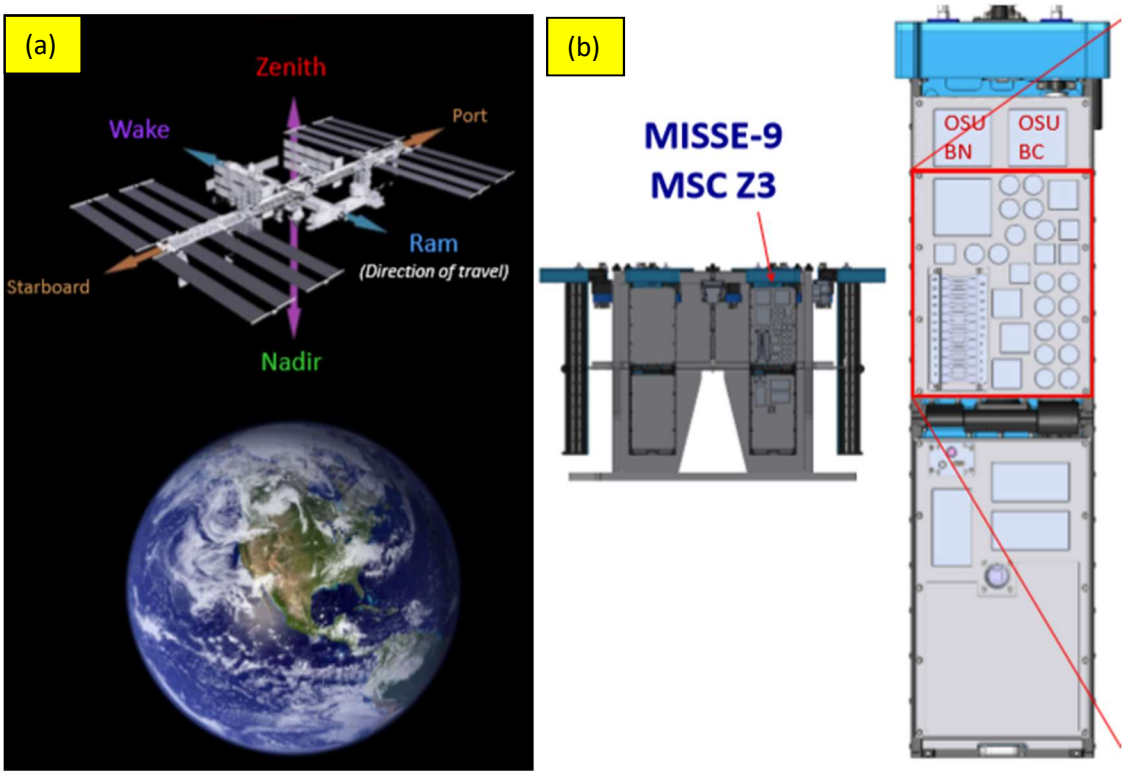

Figure 23: MISSE Sample Locations: (a) Flight Orientation and (b) Module Location

CHAPTER III

RESULTS

3.1 Characterization Tests

3.1.1 Mechanical Testing

The flexural modulus for HDPE with varying weight percentages of boron nitride is shown in figure 24. The flexural data shows that there is little variation in the flexural modulus for the varying weight percentages of boron nitride in HDPE. This could be explained by the lubricating nature of boron nitride particles, which keeps the stiff additive from forming agglomerations. This can be further confirmed by the AFM data collected.

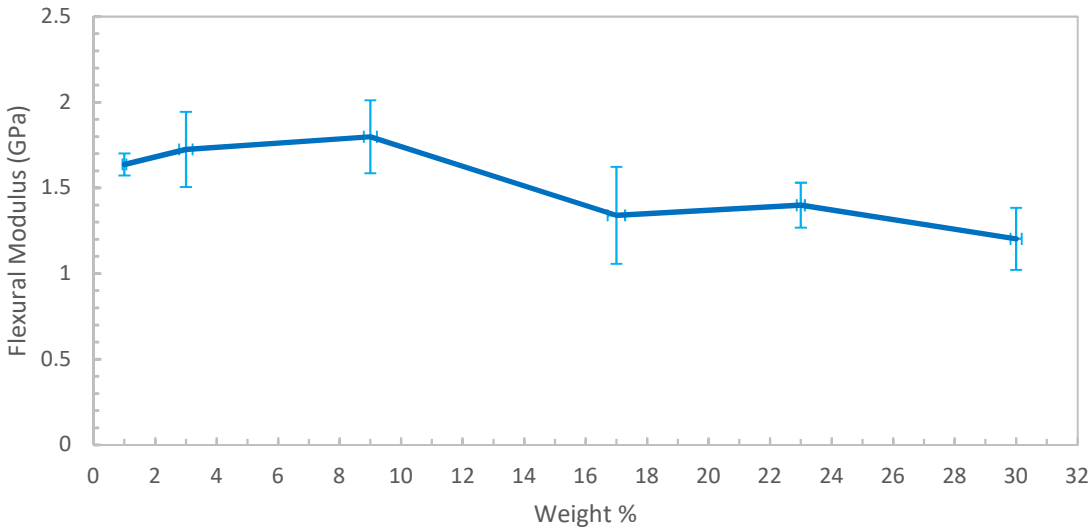

Figure 24: Change in Flexural Modulus as a Function of BN Additions to PE

The compressive modulus of HDPE with varying percentages of boron nitride was also investigated. As observed from figure 25 the compressive modulus of HDPE first decreases and then increases. This pattern of change in the compressive modulus further backs the concept that the addition of lubricating BN reduces the modulus and at higher percentages of BN, the reinforcement acts as a stiff filler. This data is also supported by the AFM data obtained.

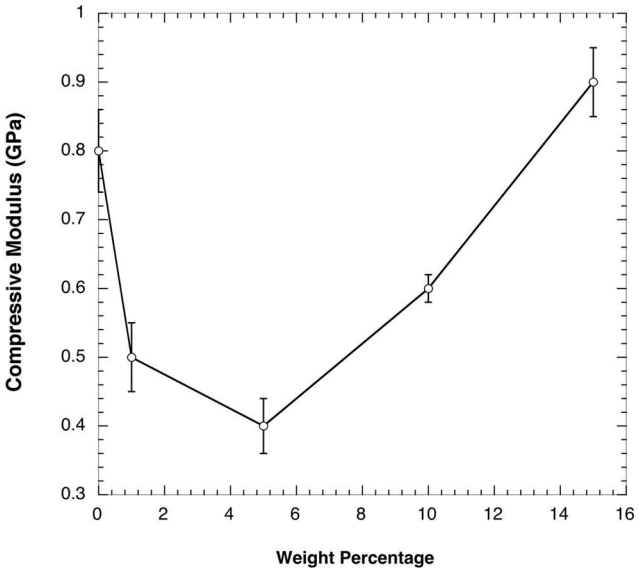

Figure 25: Compressive Properties of BN Reinforced HDPE

The tensile properties were also obtained during testing. The tensile modulus values are shown in table 3. The results show that the tensile modulus value first decreases, then as the loading of BN increases above 5 wt.% it increases again. This can be explained by the lubricating effect of BN at lower amounts, then at higher amounts, the stiffness values offset the lubricating effect. These results follow the same trend obtained from the compressive test. Overall, the ultimate tensile strength value of HDPE does not change with the incorporation of BN, which indicates the maximum load-carrying ability of the material does not change.

Table 3: Tensile Properties of BN Reinforced HDPE

Sample	Tensile Modulus (GPa)	Tensile Strength (MPa)
Pure PE	0.80 ± 0.05	39.1 ± 3.4
0.5% BN	0.72 ± 0.03	38.0 ± 4.3
5% BN	0.58 ± 0.05	37.2 ± 3.1
10% BN	0.63 ± 0.08	41.2 ± 5.1
15% BN	0.71 ± 0.03	42.3 ± 3.8

3.1.2 Atomic Force Microscopy

In contact mode, force maps were generated at each point covered in a 48 x 48 grid across a square region of 5 μm. All of these indentions were carried out in load-controlled mode. The results show the modulus map obtained after AFM indention, and the points on the modulus map represent the elastic modulus from each of the load-displacement curves. Figure 26 is the modulus map for the neat HDPE and gives an average modulus value of approximately 1 GPa.

Boron nitride was added to HDPE in different weight percentages such as 1%, 5%, 10%, and 15%. Figure 27 shows the elastic modulus map for 1 wt.% BN-HDPE sample. Based on the results, it can be seen that the boron nitride was evenly distributed throughout the HDPE. The average elastic modulus for the 1 wt.% BN-HDPE is slightly lower than the average elastic modulus for neat HDPE, at approximately 0.7 GPa. A similar decrease in elastic modulus was seen when the inclusion of BN in the sample was increased to 5 wt.%. Figure 28 shows the elastic modulus for 5 wt.% BN-HDPE to be about 0.4 GPa. The decrease in the elastic modulus for these samples could be explained by the lubricating

effect causing a reduction in stiffness. This lubricating effect is due to the sliding of the layered BN structure.

After increasing the amount of BN in HDPE, the elastic modulus begins to increase again. Figure 29 shows the elastic modulus map of 10 wt.% BN-HDPE, which gives the modulus as about 0.6 GPa. The elastic modulus increases again when the boron nitride is increased to 15 wt.%, shown in figure 30. The average elastic modulus value in this case is approximately 1 GPa, which is close to the value of the neat HDPE. This could be explained that even though the stiffness decreases with the addition of BN at lower wt.%, the higher inclusion of BN sample behaves as a stiffening material that can offset the lubricating effect. The increase in elastic modulus with the higher weight percentages of boron nitride can predict that the modulus of the PE-BN blends would increase beyond the modulus of the neat HDPE.

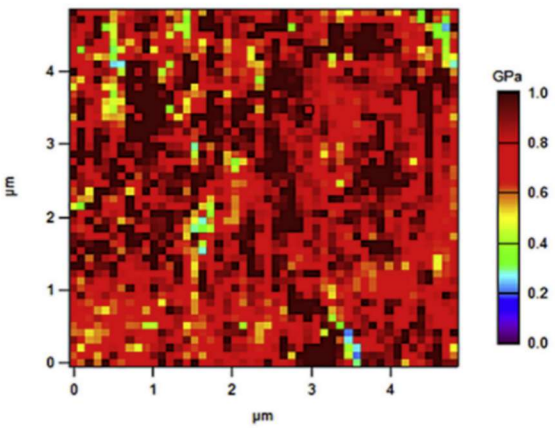

Figure 26: Elastic Modulus Map of Neat HDPE

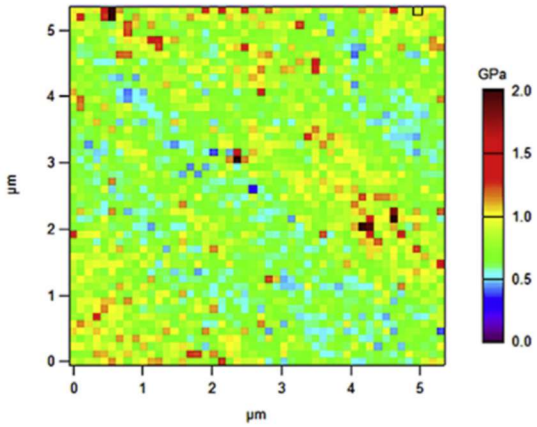

Figure 27: Elastic modulus map of 1 wt.% BN-HDPE

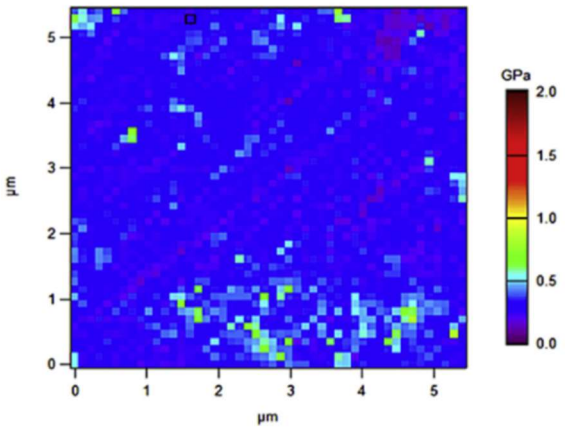

Figure 28: Elastic modulus map of 5 wt.% BN-HDPE

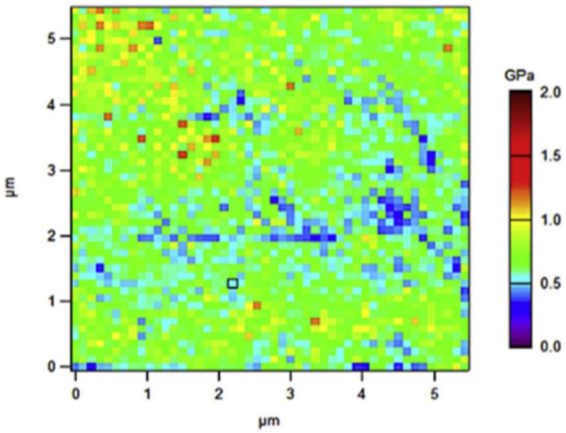

Figure 29: Elastic modulus map of 10 wt.% BN-HDPE

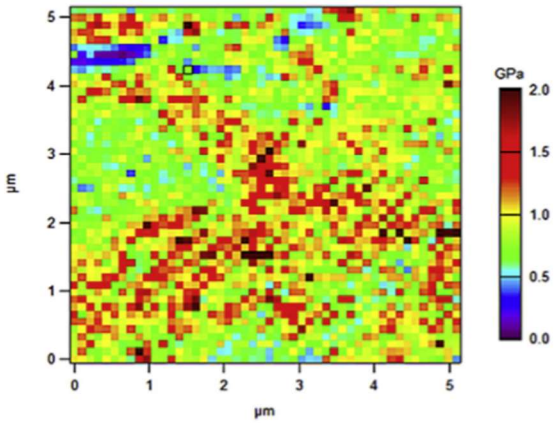

Figure 30: Elastic modulus map of 1 5 wt.% BN-HDPE

In addition to studying the elastic modulus of the varying weight percentages of boron nitride in HDPE, samples were tested based on the number of extrusions the sample went through. Samples of 30 wt.% BN-HDPE were turned into filaments by the extrusion methods mentioned. After the filament was created, some of the samples were cut off and run through the extruder a second time to produce a filament. AFM data was collected to examine the effects of extrusion on the BN-HDPE sample.

The main concern with doing multiple extrusions of the sample was agglomeration occurring when the sample is melted repeatedly. For this, the phase map of the multiple

extrusion samples was examined. The results from this study are shown in figure 31 and figure 32, for one extrusion and two extrusions, respectively. The results show that for one extrusion there is even dispersion of the boron nitride in the HDPE, however, after a second extrusion some agglomerates are formed.

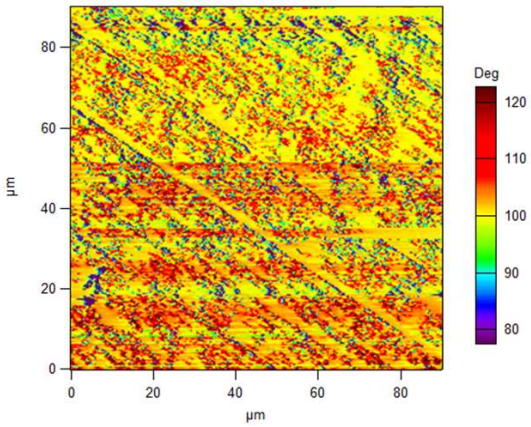

Figure 31: Phase Map for 30 wt.% BN-HDPE for One Extrusion

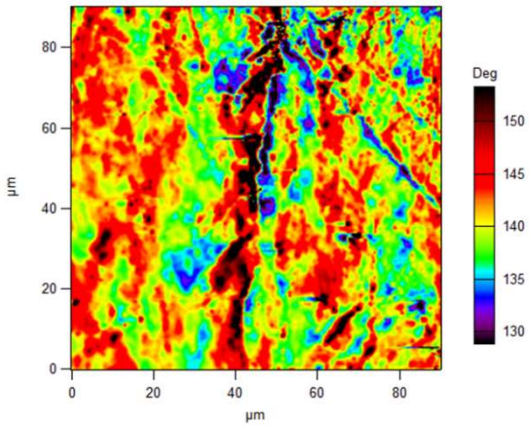

Figure 32: Phase Map for 30 wt.% BN-HDPE for Two Extrusions

3.1.3 Dynamic Mechanical Analysis

DMA was used to examine the effect of temperature on the storage modulus (E') and the loss modulus (E") for the boron nitride reinforced HDPE composites, shown in figure 33. Based on the results, it can be determined that as the temperature increases from -150°C to 100°C, the storage modulus for the boron nitride filled composites was higher than that of the neat HDPE in the glassy state (temperatures were above -50°C). This higher storage modulus in the glassy state is due to the BN filler acting as a hard segment in the polymer matrix, which prevents the molecular motions and thus increasing the stiffness of the composites. Similar behaviors were observed in the case of the loss modulus for the neat PE and BN reinforced PE.

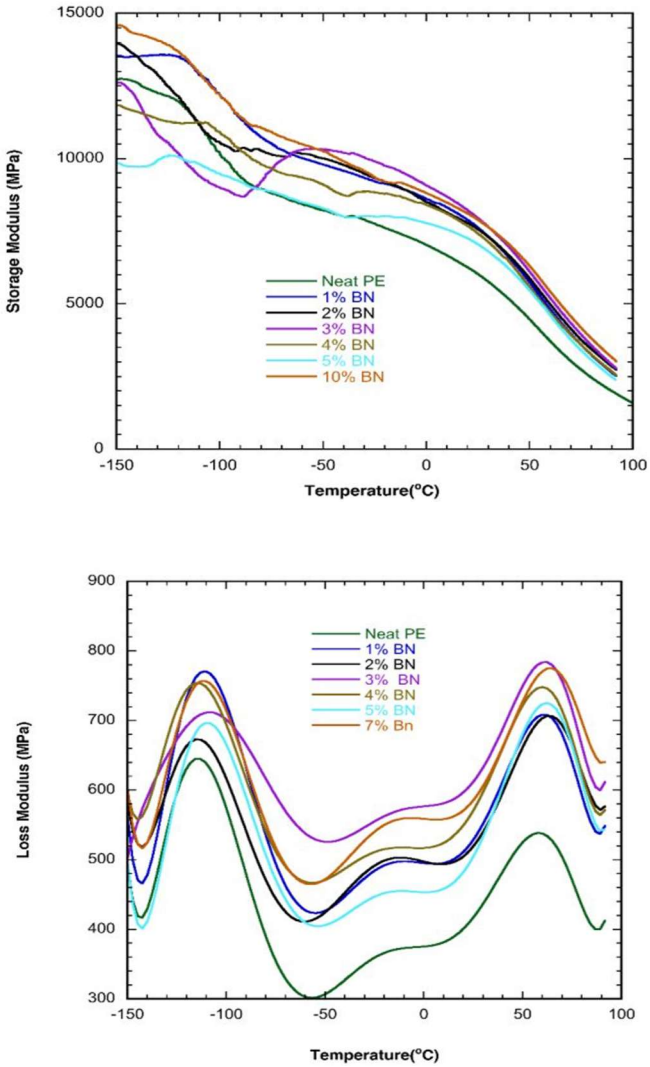

Figure 33: Storage Modulus (top) and Loss Modulus (bottom) for BN Reinforced HDPE

The damping factor, or tanδ, was also found for the BN filled PE composites, which is shown in figure 34. An increase in the damping factor was seen in the results, which can be attributed to the poor interfacial interaction between the matrix and the particles. Due to the poor interfacial interactions, high stress may be generated in the interface region, which leads to an increase in the damping factor.

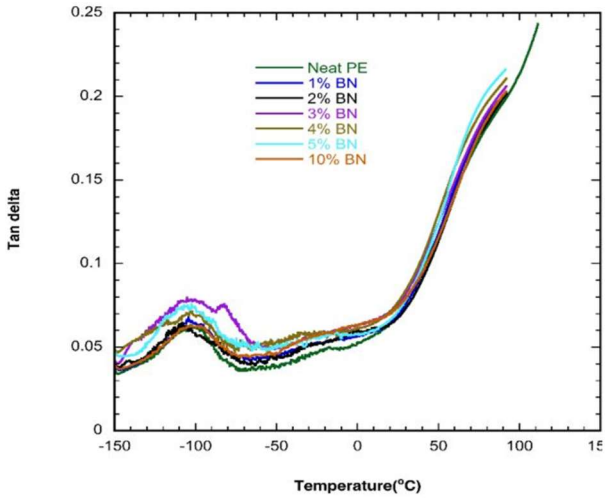

Figure 34: Damping Factor for BN Reinforced HDPE

To further investigate the effects on multiple extrusions on the samples, 30 wt.% BN-HDPE was tested after one extrusion and then two extrusions. The results, shown in figure 35 and figure 36, indicate that the number of extrusions has little to no effect on the storage modulus and loss modulus values. However, there was a slight increase in the damping factor after the second extrusion. This means that after a second extrusion, the sample is better at absorbing energy than after a single extrusion.

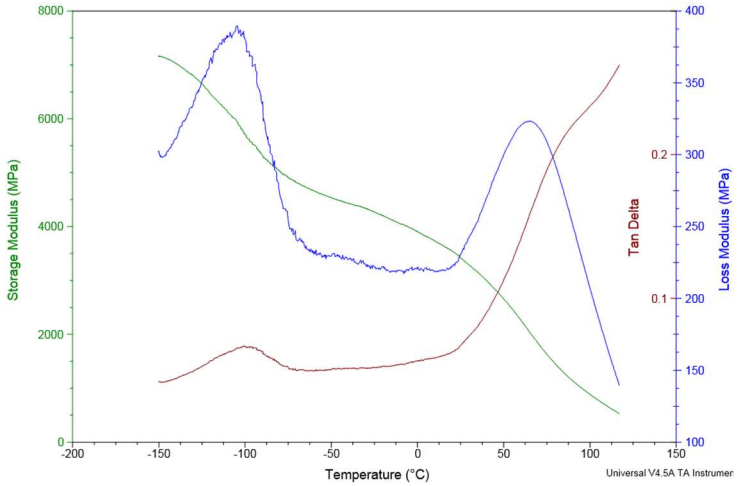

Figure 35: Storage Modulus, Loss Modulus, and Tan Delta for 30 wt.% BN-HDPE after 1 Extrusion

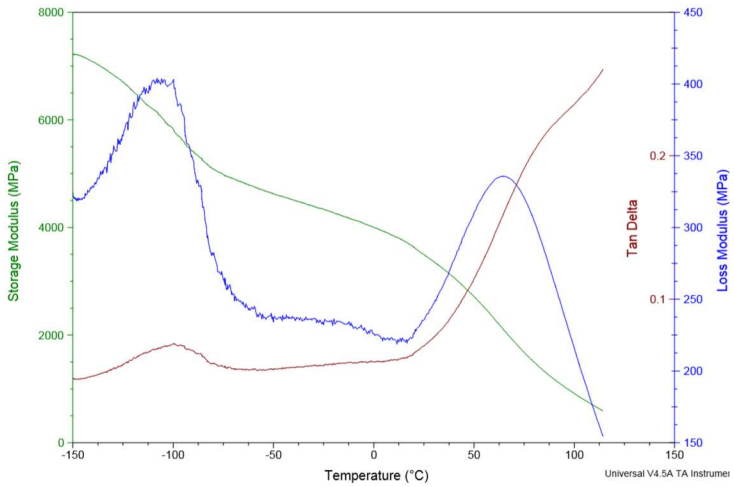

Figure 36: Storage Modulus, Loss Modulus, and Tan Delta for 30 wt.% BN-HDPE after 2 Extrusions

3.1.4 Differential Scanning Calorimetry

Differential scanning calorimetry was used to assess the melting point and crystallization point of the samples after one and two extrusions were performed. Figure 37 shows the DSC data for neat HDPE, with the crystallization temperature being approximately 116°C and the melting point at approximately 131°C.

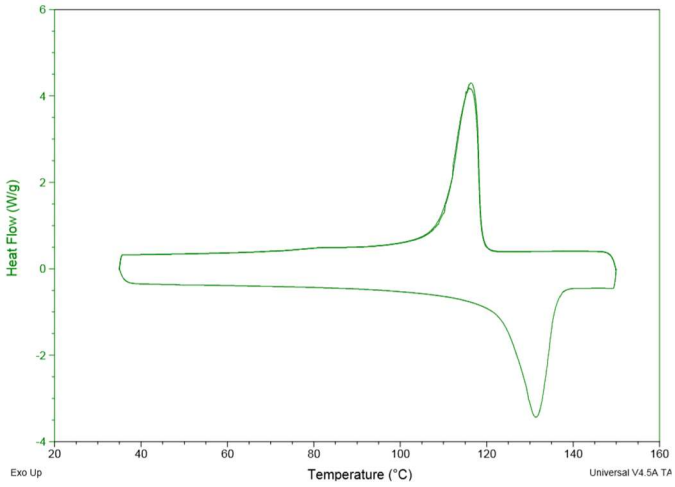

Figure 37: Melting and Crystallization Points for Neat HDPE

The DSC data is shown in figure 38 for one and two extrusions of 30 wt.% BN-HDPE, respectively. The data shows that for the melting temperature there was no change

and for the crystallization temperature there was a slight increase. The new crystallization temperature is about 122°C.

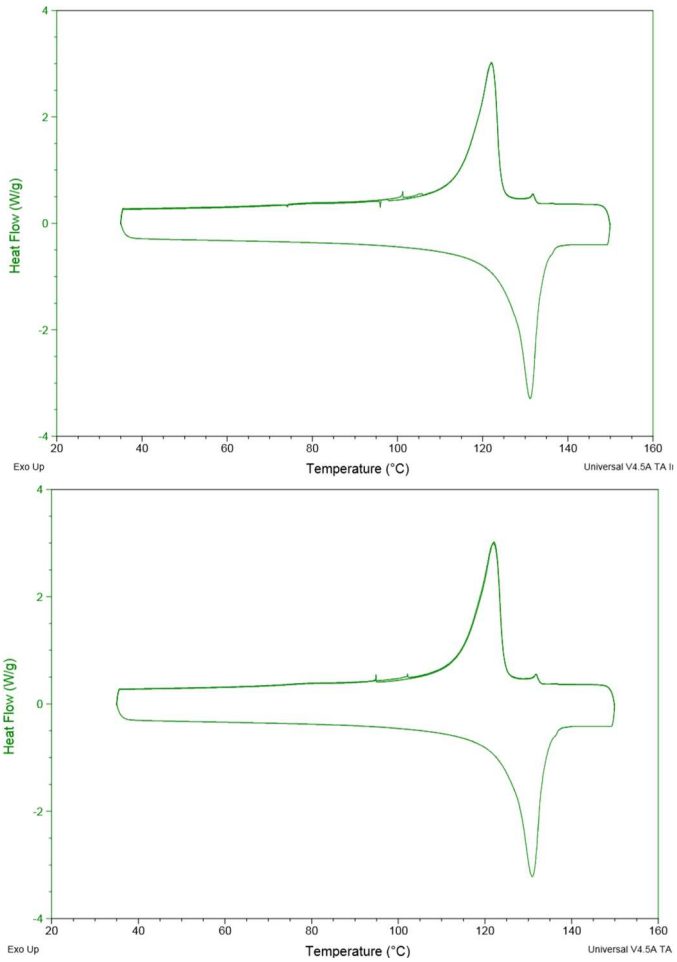

Figure 38: Melting and Crystallization Points for 30 wt.% BN-HDPE after 1 Extrusion (top) and 2 Extrusions (bottom)

3.2 Radiation Tests

3.2.1 Neutron Exposure

Neutron exposure data was obtained for HDPE containing 1%, 5%, and 30% boron nitride. The average initial activity for each of the sample types was collected and is shown in figure 39. This data indicates that as more boron nitride is added to the polyethylene, the

less radiation detected from the foil at the start of the decay. Using the initial activities, the mass absorption, or shield effectiveness, of each variance in weight percentage of boron nitride additions can be calculated. Figure 40 shows the mass absorption for each of the sample types. When these two graphs are compared to each other, they show that the lower the initial activity of the sample, the higher the shielding effectiveness. This data also indicates that the amount of boron nitride in the sample does affect the mass absorption.

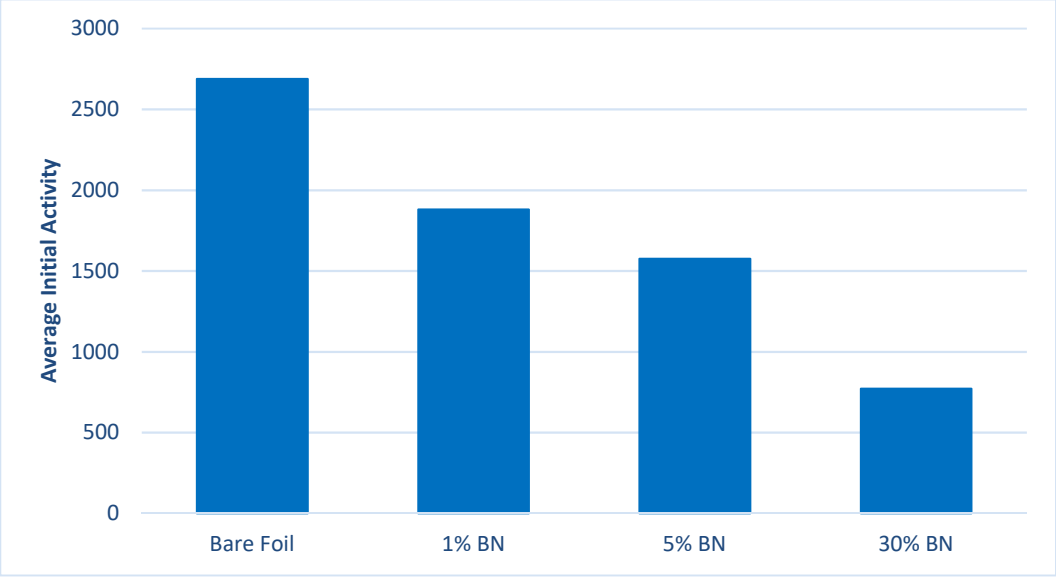

Figure 39: Average Initial Activity of BN Reinforced HDPE

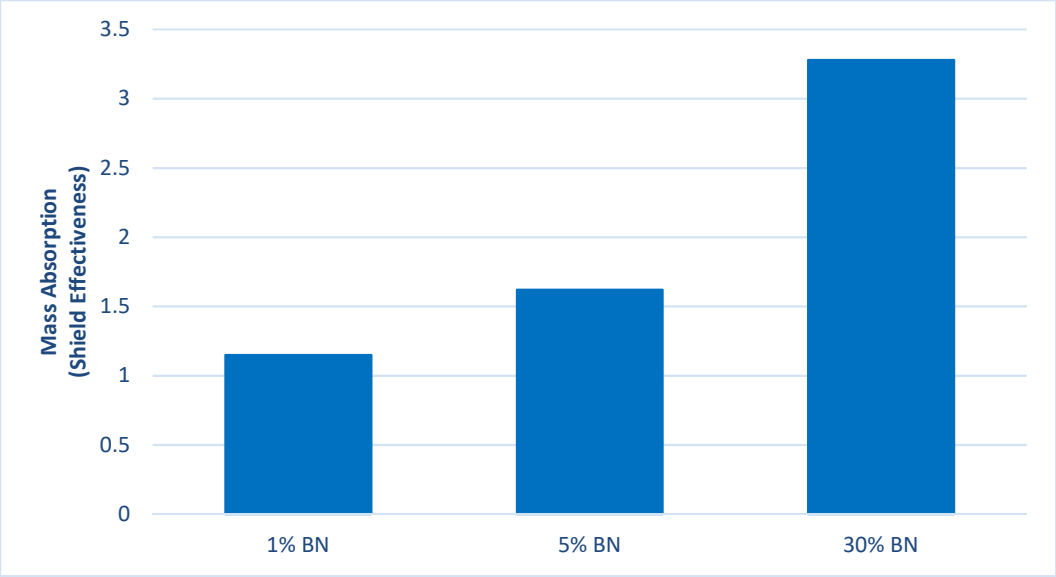

Figure 40: Mass Absorption of BN Reinforced HDPE

3.2.2 Heavy Ion Exposure

After running tests on different boron nitride containing polyethylene samples, a composite tank (SC2020) was created with 30 wt.% BN-HDPE and carbon fiber/epoxy resin. The SC2020 tank was tested after filling the tank with air and then again with water. Figure 41 shows the linear energy spectrum measured behind the SC2020 tank with and without water for the 383 MeV/n ^{16}O beam. Based on the data, having the SC2020 tank filled with air has a minimal change compared to the bare beam. This is most likely due to the tank being approximately 1 cm thick. The tank full of water shows a much more significant shift in the spectrum, which demonstrates how the water is absorbing a substantial amount of the beam's energy and shifting the lineal energy towards a higher value.

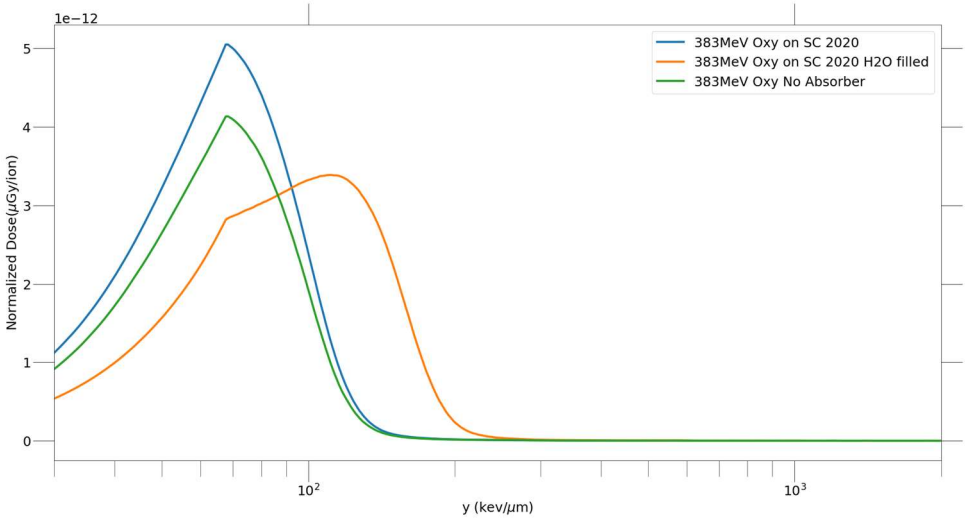

Figure 41: Lineal Energy Spectra Measured Behind the SC2020 Composite Tank Exposed to 383 MeV/n ^{16}O

Figure 42 shows the lineal energy spectrum measured behind the SC2020 tank with and without water for the 422 MeV/n ^{56}Fe beam. Again, due to the 1 cm thickness of the tank, the tank alone does little to stop the ^{56}Fe beam. However, once water is added to the tank there is an extreme drop in the amount absorbed, leading to almost complete shielding. For both beam types, this is a good representation of how water can be used as a multifunctional shielding material and how SC2020 composite tanks can effectively hold water as both a shielding material and as a consumable abroad a manned spacecraft.

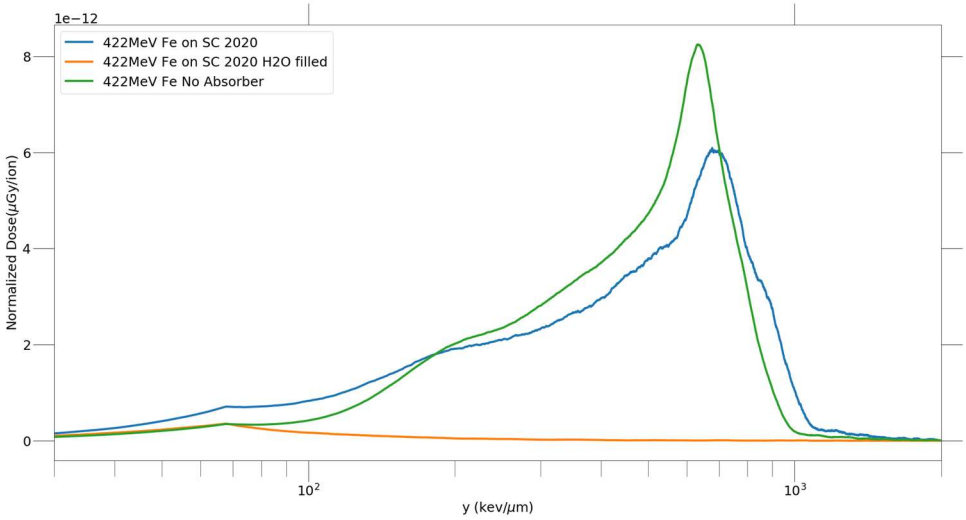

Figure 42: Lineal Energy Spectra Measured Behind the SC2020 Composite Tank Exposed to 422 MeV/n ^{56}Fe

3.2.3 Materials on the International Space Station Experiments (MISSE)

During the transportation of the MISSE-9 samples, the TLDs fell out of the sample blocks, which caused there to be no results collected. There was nothing to analyze for that experiment. Since the MISSE-11 experiment did not return from the International Space Station until the spring of 2020 and then needed to be returned to Oklahoma State University, the data from the TLDs is currently being analyzed. The OSU Radiation Physics Lab plans to extract and analyze this data in the near future.

CHAPTER IV

DISCUSSION

4.1 Mechanical Properties

The characterization tests conducted during this experiment can be divided into two groups for analysis. The first group is based on the variation of the boron nitride additive in the polyethylene composite and the second group is based on the number of extrusions a boron nitride-polyethylene composite experienced.

The first set of data is based on the varying weight percent of boron nitride in the polyethylene composite. The first three tests considered were the flexural modulus, compressive modulus, and tensile properties. The flexural modulus showed little variation when changing the amount of boron nitride present. While the compressive modulus and tensile properties did show a change. Both decrease initially at lower amounts of boron nitride, then above approximately 5 wt.% BN, both moduli show an increase. All three of these results can be explained by the lubricating effects of hexagonal boron nitride that it possesses from having a structure similar to that of graphite. At the higher amounts of boron nitride, the reinforcement acts as a stiff filler, which causes the properties to increase. The results of these tests were then backed using AFM. AFM results show that at lower amounts of BN in HDPE, there was a decrease in the elastic modulus. Then as more BN was added, above 5 wt.%, the elastic modulus increases again. The storage modulus, loss

modulus, and damping factor were also examined using DMA. The results show that for the storage modulus and loss modulus, the boron nitride filled composites have a higher value than for the neat HDPE. This is also seen for the damping factor. All of these tests combined leads to the conclusion that including a higher amount of boron nitride in the polyethylene composite will increase the mechanical properties of the structure. This conclusion helped in deciding that 30% BN-HDPE samples were to be used in further research. Part of this decision was obtained from the mechanical property analysis, and the other part was the physical restrictions associated with mixing these two components. When mixing the two components, the polyethylene has a limited amount of boron nitride powder that it can hold. 30 wt.% BN was the highest amount that could be fully contained in the HDPE. 35 wt.% or higher led to some of the powder not being absorbed into the HDPE, which would be an inaccurate representation of the wt.% for the composite.

The second set of data was related to the number of extrusions that the composite material was exposed to. Multiple extrusions were considered to help in creating a more uniform filament when producing the composite tanks. These filaments were tested to ensure that heating the sample multiple times for extrusion would not interfere with the properties of the sample. The first test done was testing the phase maps using AFM to ensure that agglomerates weren't forming. After testing both the single extrusion and double extrusion 30 wt.% BN samples, it was determined that doing multiple extrusions led to the boron nitride not being evenly dispersed throughout the sample. Doing multiple extrusions on the composite sample had little to no effect on the storage modulus and loss modulus obtained using DMA and the melting temperature obtained using DSC. There did appear to be a slight increase in the damping factor obtained using DMA and the

crystallization temperature using DSC though. Overall, for the construction of the tanks for this experiment, it was determined that using a single extrusion would be the best course of action.

4.2 Radiation Properties

The radiation tests were designed to ensure that by adding the additive to the polyethylene sample, the additive wouldn't hinder the shielding abilities of the material. The first round of radiation tests was the neutron exposure experiment. These were designed to test if boron nitride would add help in shielding against secondary neutrons that could be created in a space shuttle. The neutron exposure results showed that as the amount of boron nitride was increased in the polyethylene sample, there was a lower average initial activity that results in a higher shield effectiveness. This indicates that the boron nitride can help in reducing the number of secondary neutrons that are created due to GCR from reaching the astronauts.

The HIMAC tests were used to evaluate the potential for the all composite PE-BN tank. A 30% BN-PE tank was tested using two different ionization beams. The results for this proved that the PE-BN tank filled with air was slightly able to shield against different radiation types. The tank filled with water was able to significantly shield against the radiation types. For the Fe beam, the tank filled with water was able to reduce the ionization to almost zero. These results prove that if these tanks were to be implemented into the space station or space shuttles they could be used as lightweight containers for items already necessary and protect the astronauts from the harms of radiation.

CHAPTER V

CONCLUSIONS

When it comes to space missions, there is always a goal to save money, while also keeping up the integrity of the space shuttles. One way of doing this is to develop new materials that are lighter and more cost-effective but can still achieve what is needed. Composite materials have led to major developments in accomplishing these goals. With the development of the boron nitride-polyethylene composite material, this could lead to changes in how the space shuttles are developed. Polyethylene is the standard for space radiation shielding, so to create a material that still has the radiation shielding properties of polyethylene but increases the mechanical properties is a huge step forward in the aerospace industry. BN-PE composite tanks could be used to replace storage containers on the ISS, such as the water and urine storage units in the water recycling process. This would replace the heavier materials currently used and would also provide radiation protection along the ISS.

The tanks would also have the ability to reduce the weight associated with extra loads on space shuttles, such as vehicles. With the desire to return to the Moon, and eventually Mars, vehicles will be needed to explore these surfaces, so finding ways to reduce the weight of them would result in fewer fuel costs associated with the missions. The tanks could be used to replace the fuel tanks on the vehicles and reduce the weight.

Further research could be done to modify the material for uses such as habitats or using the filament for integration into spacesuits. Both applications would help in protecting astronauts from the radiation experienced in space.

REFERENCES

[1] NASA, "In Their Footsteps: The Mercury 7," 19 December 2005. [Online]. Available: https://www.nasa.gov/centers/kennedy/about/history/mercury7.html.

[2] NASA, "July 20, 1969: One Giant Leap for Mankind," NASA, 20 July 2019. [Online]. Available: https://www.nasa.gov/mission_pages/apollo/apollo11.html.

[3] NASA, "Space Station 20th: Historical Origins of ISS," NASA, 23 January 2020. [Online]. Available: https://www.nasa.gov/feature/space-station-20th-historical-origins-of-iss.

[4] D. M. Harland, "Encyclopedia Britannica," Encyclopedia Britannica, inc., 31 December 2019. [Online]. Available: https://www.britannica.com/science/Constellation-program.

[5] D. S. A. Thibeault, D. C. C. Fay, S. E. Lowther, K. D. Earle, D. G. Sauti, D. J. H. Kang, D. C. Park and A. M. McMullen, "Radiation Shielding Materials Containing Hydrogen, Boron, and Nitrogen: Systematic Computational and Experimental Study - Phase 1," NASA, Hampton, 2012.

[6] J. Rask, D. W. Vercoutere, B. J. Navarro and A. Krause, *Radiation Educator Guide – Introduction and Module 1: Radiation.*

[7] J. W. Wilson, F. A. Cucinotta, J. Miller, J. L. Shinn, S. A. Thibeault, R. C. Singleterry, L. C. Simonsen and M. H. Kim, "Materials for Shielding Astronauts from the Hazards of Space Radiations," *Symposium JJ - Materials in Space Science, Technology & Exploration,* vol. 551, 1998.

[8] J. L. Barth, "Space and Atmospheric Environments: From Low Earth Orbits to Deep Space," *Protection of Materials and Structures from Space Environments,* vol. 5, 2004.

[9] "Learning Launchers: Radiation," NASA, [Online]. Available: https://www.nasa.gov/audience/foreducators/stem-on-station/learning_launchers_radiation.

[10] P. L. Barry, "Plastic Spaceships," NASA, 25 August 2005. [Online]. Available: https://science.nasa.gov/science-news/science-at-nasa/2005/25aug_plasticspaceships#:~:text=Plastic%20is%20an%20appealing%20alternative,15%25%20better%20for%20cosmic%20rays.&text=The%20advantage%20of%20plastic%2Dlike,materials%20like%20aluminum%20or%20lead. [Accessed July 2020].

[11] Z. Soltani, A. Beigzadeh, F. Ziaie and E. Asadi, "Effect of particle size and percentages of Boron carbide on the thermal neutron radiation shielding properties of HDPE/B4C composite: Experimental and simulation studies," *Radiation Physics and Chemistry,* vol. 127, pp. 182-187, 2016.

[12] A. Emmanuel and J. Raghavan, "Influence of structure on radiation shielding effectiveness of graphite fiber reinforced polyethylene composite," *Advances in Space Research,* vol. 56, pp. 1288-1296, 2015.

[13] M. E. Mahmoud, A. M. El-Khatib, M. S. Badawi, A. R. Rashad, R. M. El-Sharkawy and A. A. Thabet, "Fabrication, characterization and gamma rays shielding properties of nano and micro lead oxide-dispersed-high density polyethylene composites," *Radiation Physics and Chemistry,* vol. 145, pp. 160-173, 2018.

[14] C. Harrison, S. Weaver, C. Bertelsen, E. Burgett, N. Hertel and E. Grulke, "Polyethylene/Boron Nitride Composites for Space Radiation Shielding," *Journal of Applied Polymer Science,* vol. 109, pp. 2529-2538, 2008.

[15] M. Scott and R. Vaidyanathan, "Radiation Smart Structures with H-rich Nanostructured Multifunctional Materials," Tulsa, 2017.

[16] K. K. de Groh and B. A. Banks, "The MISSE-9 Polymers and Composites Experiment Being Flown on the MISSE-Flight Facility," in *International Space Station Research and Development Conference*, Washington, D.C., 2017.

[17] C. Harrison, E. Burgett, N. Hertel and E. Grulke, "Polyethylene/Boron Composites for

Radiation Shielding Applications," in *American Institute of Physics Conference*, 2008.

APPENDICES

Table AI: Density of media considered in the simulation and thickness of 5.0 g/cm^2 media converted to cm

Medium	Density (g/cm^3)	Thickness equivalent to 5.0 g/cm^2 of medium (cm)
Pure PE	0.940	5.319
PE with 10% BN	0.995	5.025
PE with 25% BN	1.091	4.585
PE with 50% BN	1.299	3.850
PE with 75% BN	1.605	3.116
PE with 90% BN	1.869	2.675
Pure BN	2.100	2.381

Figure AI: Comparison of LET spectra measured at different depths within polyethylene with varying amounts of boron nitride by mass for simulated exposures to a beam of 1 GeV/n ^{28}Si

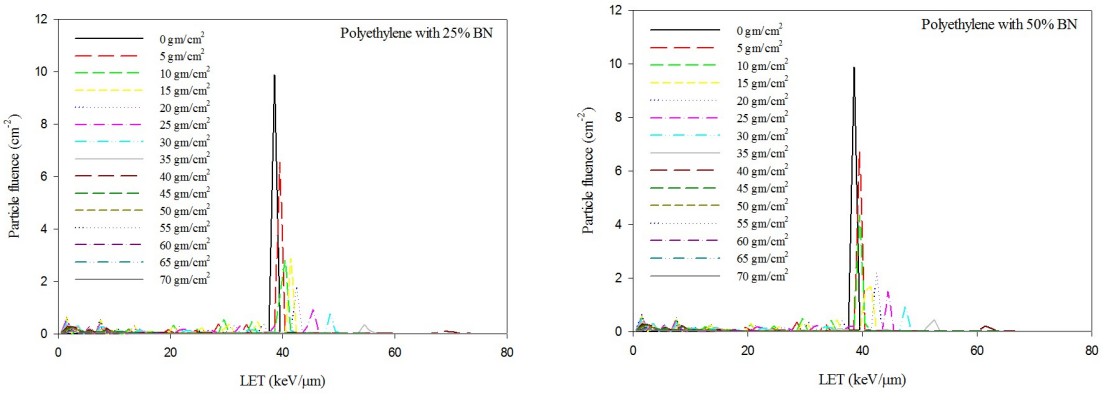

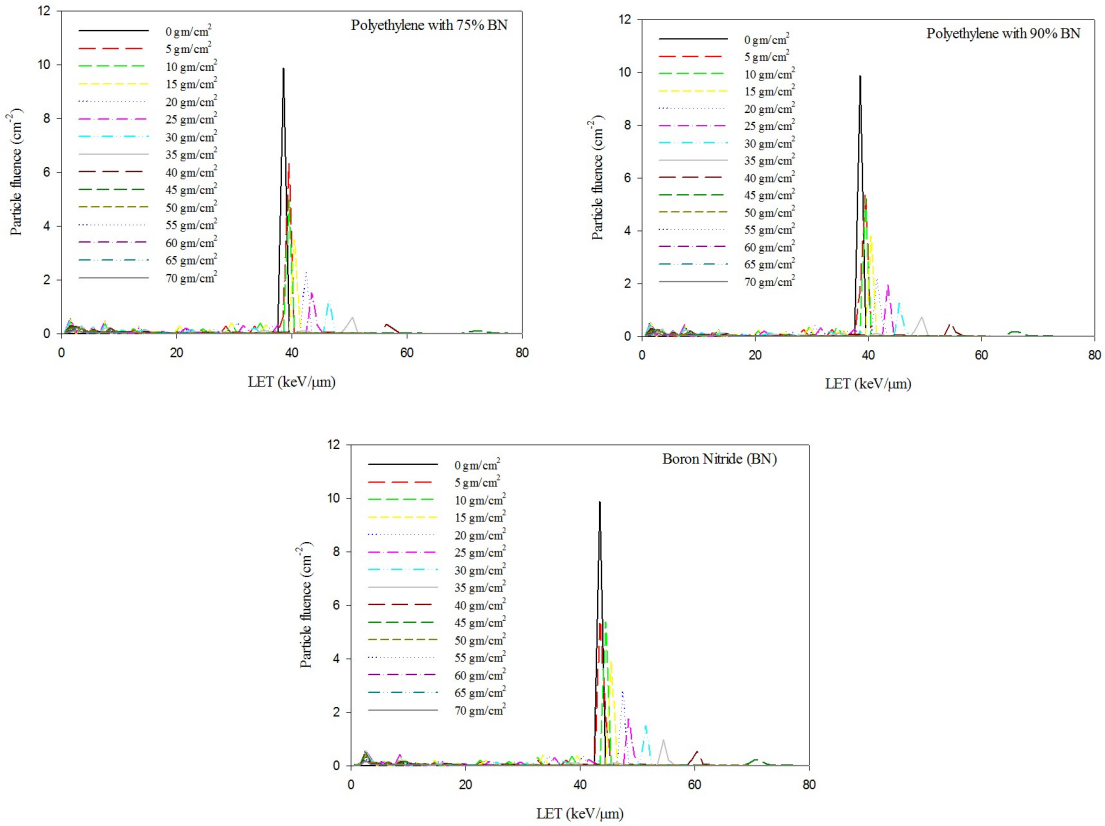

Table AII: Absorbed dose calculated using the LET spectra for simulated exposures to a beam of 1 GeV/n ^{28}Si

Depth (g/cm^2)	Total absorbed dose using LET spectra (Gy × 10^{-7})						
	Pure PE	PE with 10% BN	PE with 25% BN	PE with 50% BN	PE with 75% BN	PE with 90% BN	Pure BN
0	6.896	6.104	6.105	6.103	6.104	6.104	6.897
5	5.294	4.730	4.783	4.860	4.925	4.962	5.578
10	4.077	3.672	3.737	3.803	3.923	4.006	4.573
15	3.162	2.869	2.962	3.069	3.184	3.285	3.771
20	2.495	2.275	2.349	2.484	2.635	2.709	3.156
25	2.011	1.832	1.920	2.039	2.163	2.263	2.619
30	1.667	1.520	1.590	1.708	1.827	1.906	2.234
35	1.455	1.323	1.378	1.472	1.576	1.657	1.932
40	1.420	1.268	1.282	1.329	1.402	1.467	1.707
45	0.8785	0.8584	1.313	1.445	1.363	1.391	1.600
50	0.4392	0.4299	0.5203	0.7159	1.211	1.680	1.782
55	0.2413	0.2362	0.2767	0.3662	0.5041	0.6197	0.8033
60	0.1447	0.1360	0.1617	0.2050	0.2785	0.3245	0.4239
65	0.09043	0.08676	0.1023	0.1298	0.1713	0.1974	0.2486

70	0.05875	0.05367	0.06583	0.08529	0.1120	0.1298	0.1633

Table AIII: Absorbed dose normalized by the absorbed dose at 0 g/cm^2 for simulated exposures to a beam of 1 GeV/n ^{28}Si

Depth (g/cm^2)	Total absorbed dose using LET spectra (Normalized)						
	Pure PE	PE with 10% BN	PE with 25% BN	PE with 50% BN	PE with 75% BN	PE with 90% BN	Pure BN
0	1.000	1.000	1.000	1.000	1.000	1.000	1.000
5	0.768	0.775	0.784	0.796	0.807	0.813	0.809
10	0.591	0.602	0.612	0.623	0.643	0.656	0.663
15	0.458	0.470	0.485	0.503	0.522	0.538	0.547
20	0.362	0.373	0.385	0.407	0.432	0.444	0.458
25	0.292	0.300	0.315	0.334	0.354	0.371	0.380
30	0.242	0.249	0.260	0.280	0.299	0.312	0.324
35	0.211	0.217	0.226	0.241	0.258	0.271	0.208
40	0.206	0.208	0.210	0.218	0.230	0.240	0.247
45	0.127	0.141	0.215	0.237	0.223	0.228	0.232
50	0.064	0.070	0.085	0.117	0.198	0.275	0.258
55	0.035	0.039	0.045	0.060	0.083	0.102	0.116
60	0.021	0.022	0.026	0.034	0.046	0.053	0.061
65	0.013	0.014	0.017	0.021	0.028	0.032	0.036
70	0.009	0.009	0.011	0.014	0.018	0.021	0.024

Table AIV: Equivalent dose calculated using LET spectra (Sv) for simulated exposures to a beam of 1 GeV/n ^{28}Si

Depth (g/cm^2)	Equivalent dose using LET spectra (Sv $\times 10^{-6}$)						
	Pure PE	PE with 10% BN	PE with 25% BN	PE with 50% BN	PE with 75% BN	PE with 90% BN	Pure BN
0	7.856	5.978	5.979	5.977	5.978	5.978	7.857
5	5.791	4.475	4.550	4.657	4.744	4.785	6.173
10	4.278	3.350	3.417	3.470	3.629	3.743	4.978
15	3.188	2.532	2.653	2.776	2.904	3.040	4.068
20	2.477	1.974	2.048	2.227	2.428	2.497	3.445
25	2.008	1.595	1.697	1.836	1.979	2.110	2.843
30	1.737	1.376	1.447	1.582	1.723	1.812	2.494
35	1.695	1.328	1.366	1.455	1.561	1.658	2.236
40	2.298	1.720	1.594	1.527	1.542	1.604	2.139
45	1.223	1.157	1.860	2.550	1.931	1.841	2.351
50	0.4782	0.4570	0.5998	0.9516	1.743	3.283	3.652

55	0.2047	0.1950	0.2455	0.3778	0.5962	0.8153	1.179
60	0.1009	0.08691	0.1098	0.1612	0.2566	0.3310	0.4884
65	0.05625	0.04953	0.06050	0.08460	0.1266	0.1619	0.2328
70	0.03556	0.02539	0.03577	0.04876	0.07365	0.09158	0.1303

Table AV: Equivalent dose calculated using LET spectra, normalized by the equivalent dose at 0 g/cm^2 for simulated exposures to a beam of 1 GeV/n ^{28}Si

Depth (g/cm^2)	Equivalent dose using LET spectra (Normalized)						
	Pure PE	PE with 10% BN	PE with 25% BN	PE with 50% BN	PE with 75% BN	PE with 90% BN	Pure BN
0	1.000	1.000	1.000	1.000	1.000	1.000	1.000
5	0.737	0.749	0.761	0.779	0.794	0.800	0.786
10	0.544	0.560	0.572	0.581	0.607	0.626	0.634
15	0.406	0.423	0.444	0.464	0.486	0.508	0.518
20	0.315	0.330	0.343	0.373	0.406	0.418	0.438
25	0.256	0.267	0.284	0.307	0.331	0.353	0.362
30	0.221	0.230	0.242	0.265	0.288	0.303	0.317
35	0.216	0.222	0.229	0.243	0.261	0.277	0.285
40	0.293	0.288	0.267	0.255	0.258	0.268	0.272
45	0.156	0.194	0.311	0.427	0.323	0.308	0.299
50	0.061	0.076	0.100	0.159	0.292	0.549	0.465
55	0.026	0.033	0.041	0.063	0.100	0.136	0.150
60	0.013	0.015	0.018	0.027	0.043	0.055	0.062
65	0.007	0.008	0.010	0.014	0.021	0.027	0.030
70	0.005	0.004	0.006	0.008	0.012	0.015	0.017

Table AVI: Percent fraction of ^{28}Si ions at different depths within various media

Depth (g/cm^2)	Percent Fraction of ^{28}Si ions						
	Pure PE	PE with 10% BN	PE with 25% BN	PE with 50% BN	PE with 75% BN	PE with 90% BN	Pure BN
0	0.36	0.33	0.36	0.35	0.34	0.36	0.37
10	30.09	28.92	27.16	24.40	21.57	19.60	18.41
15	49.65	48.20	45.76	42.01	37.59	34.62	32.56
20	63.26	61.79	59.15	54.85	49.90	46.26	44.09
25	72.70	71.35	68.77	64.42	59.44	55.71	53.34
30	79.43	78.26	75.93	71.81	66.90	63.34	60.86
35	84.23	83.29	81.31	77.89	72.83	69.45	66.95
40	88.01	86.94	85.29	81.76	77.70	74.25	72.01
45	90.50	89.67	88.28	85.13	81.55	78.21	76.27

50	100.00	100.00	100.00	88.27	84.73	81.56	79.48
55	100.00	100.00	100.00	100.00	100.00	85.01	82.51
60	100.00	100.00	100.00	100.00	100.00	100.00	100.00
65	100.00	100.00	100.00	100.00	100.00	100.00	100.00
70	100.00	100.00	100.00	100.00	100.00	100.00	100.00

Figure AII: Comparison of LET spectra measured at different depths within polyethylene containing varying amounts of boron nitride by mass following simulated exposure to a 1 GeV/n ^{56}Fe beam

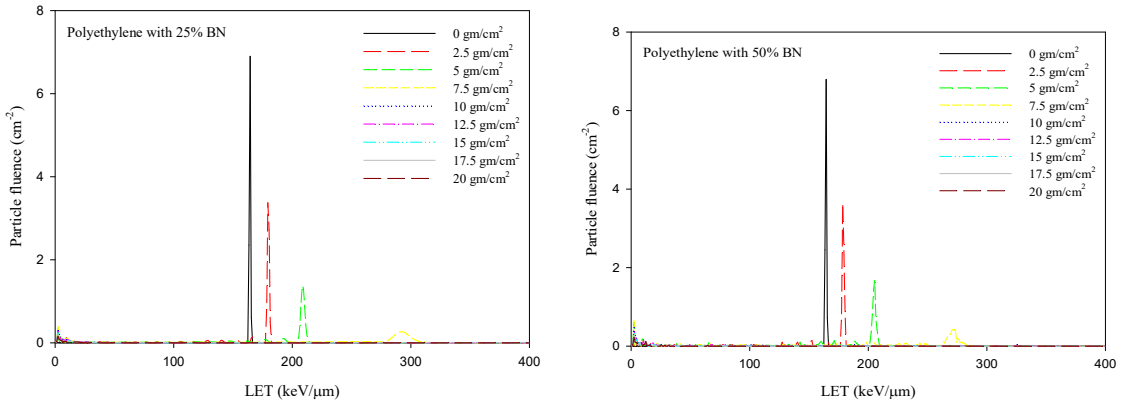

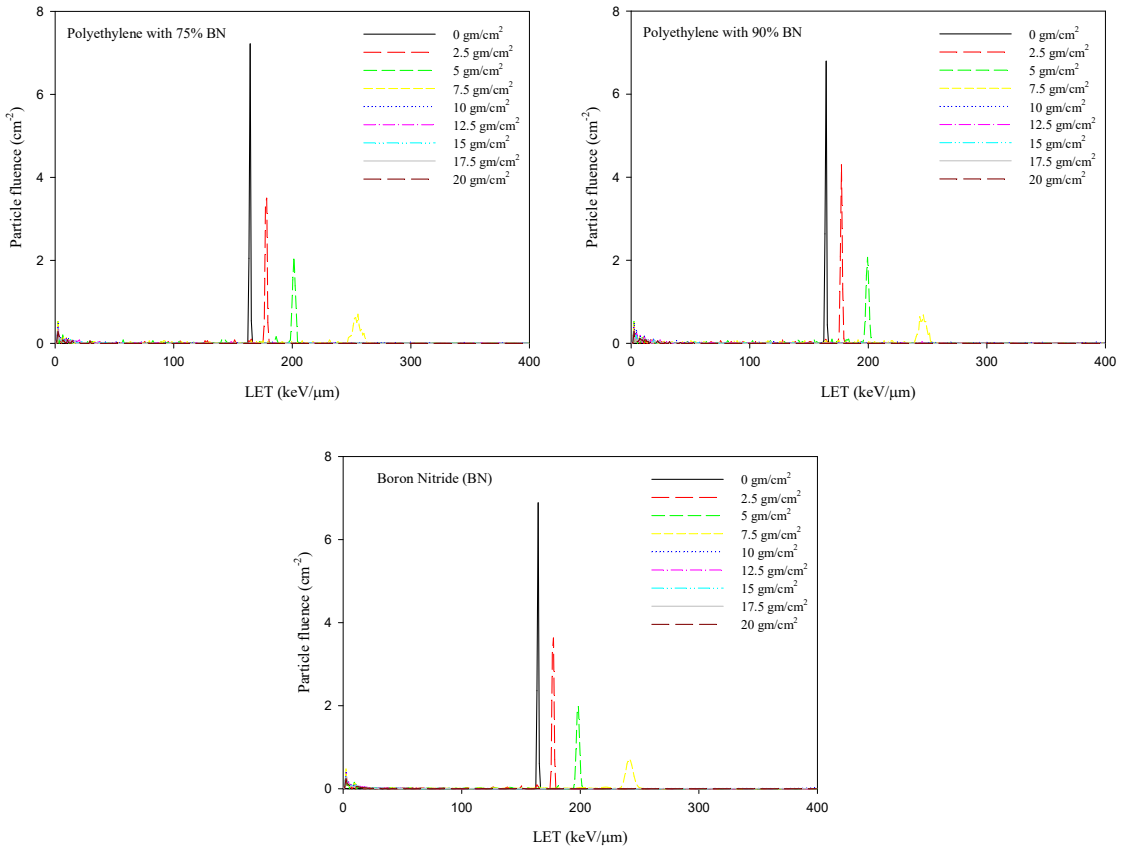

Table AVII: Absorbed dose calculated using the LET spectra following simulated exposure to a 1 GeV/n ^{56}Fe beam

Depth (g/cm^2)	Total absorbed dose using LET spectra (Gy × 10^{-7})						
	Pure PE	PE with 10% BN	PE with 25% BN	PE with 50% BN	PE with 75% BN	PE with 90% BN	Pure BN
0	29.40	26.06	26.07	26.29	26.00	26.18	26.05
2.5	28.58	25.33	25.30	25.45	25.24	25.11	25.15
5	29.89	26.36	26.15	25.79	25.83	25.19	25.29
7.5	38.92	33.90	32.36	29.84	28.89	28.06	27.70
10	3.229	3.342	3.970	6.466	7.568	9.798	12.11
12.5	1.017	0.9878	1.152	1.698	2.039	2.206	2.542
15	0.4541	0.4327	0.5105	0.6337	0.7240	0.8999	1.124
17.5	0.2563	0.2419	0.2780	0.2745	0.2372	0.6899	0.5998
20	0.1644	0.1486	0.1744	0.1834	0.1821	0.3119	0.3653

Table AVIII: Absorbed dose normalized by the absorbed dose at 0 g/cm^2 following simulated exposure to a 1 GeV/n ^{56}Fe beam

Depth (g/cm^2)	Total absorbed dose using LET spectra (Normalized)						
	Pure PE	PE with 10% BN	PE with 25% BN	PE with 50% BN	PE with 75% BN	PE with 90% BN	Pure BN
0	1.000	1.000	1.000	1.000	1.000	1.000	1.000
2.5	0.972	0.972	0.970	0.968	0.971	0.959	0.965
5	1.016	1.011	1.003	0.981	0.993	0.962	0.971
7.5	1.323	1.301	1.241	1.135	1.111	1.072	1.063
10	0.110	0.128	0.152	0.246	0.291	0.374	0.465
12.5	0.035	0.038	0.044	0.065	0.078	0.084	0.098
15	0.015	0.017	0.020	0.024	0.028	0.034	0.043
17.5	0.009	0.009	0.011	0.010	0.009	0.026	0.023
20	0.006	0.006	0.007	0.007	0.007	0.012	0.014

Table AIX: Equivalent dose calculated using LET spectra (Sv) following simulated exposure to a 1 GeV/n ^{56}Fe beam

Depth (g/cm^2)	Equivalent dose using LET spectra (Sv $\times$ 10^{-6})						
	Pure PE	PE with 10% BN	PE with 25% BN	PE with 50% BN	PE with 75% BN	PE with 90% BN	Pure BN
0	64.80	61.00	61.02	61.52	60.87	61.28	60.97
2.5	60.87	57.11	57.06	57.48	56.98	56.69	56.81
5	59.75	55.77	55.49	55.23	55.27	54.21	54.35
7.5	65.77	61.29	59.77	57.39	56.12	55.30	54.74
10	6.148	6.394	7.585	12.80	14.40	17.73	21.74
12.5	1.756	1.687	2.013	3.155	3.879	4.127	4.724
15	0.6340	0.5890	0.7212	0.9941	1.162	1.394	1.878
17.5	0.2837	0.2614	0.3081	0.1973	0.1953	1.026	0.8412
20	0.1520	0.1282	0.1554	0.09476	0.1215	0.2483	0.4255

Table AX: Equivalent dose calculated using LET spectra, normalized by the equivalent dose at 0 g/cm^2 following simulated exposure to a 1 GeV/n ^{56}Fe beam

Depth (g/cm^2)	Equivalent dose using LET spectra (Normalized)						
	Pure PE	PE with 10% BN	PE with 25% BN	PE with 50% BN	PE with 75% BN	PE with 90% BN	Pure BN
0	1.000	1.000	1.000	1.000	1.000	1.000	1.000
2.5	0.939	0.936	0.935	0.934	0.936	0.925	0.932

5	0.922	0.914	0.909	0.898	0.908	0.885	0.891
7.5	1.015	1.005	0.979	0.933	0.922	0.902	0.898
10	0.095	0.105	0.124	0.208	0.237	0.289	0.357
12.5	0.027	0.028	0.033	0.051	0.064	0.067	0.077
15	0.010	0.010	0.012	0.016	0.019	0.023	0.031
17.5	0.004	0.004	0.005	0.003	0.003	0.017	0.014
20	0.002	0.002	0.003	0.002	0.002	0.004	0.007

Table AXI: Percent fraction of ^{56}Fe ions at different depths within various media

Depth (g/cm^2)	**Percent Fraction of ^{56}Fe ions**						
	Pure PE	**PE with 10% BN**	**PE with 25% BN**	**PE with 50% BN**	**PE with 75% BN**	**PE with 90% BN**	**Pure BN**
0	0.67	0.67	0.65	0.40	1.01	0.20	0.66
2.5	26.98	26.13	25.09	24.65	20.48	21.92	19.23
5	45.65	44.24	42.61	45.96	34.33	38.46	33.74
7.5	57.41	55.57	54.47	61.60	48.24	50.00	45.25
10	100.00	100.00	100.00	100.00	100.00	100.00	100.00
12.5	100.00	100.00	100.00	100.00	100.00	100.00	100.00
15	100.00	100.00	100.00	100.00	100.00	100.00	100.00
17.5	100.00	100.00	100.00	100.00	100.00	100.00	100.00
20	100.00	100.00	100.00	100.00	100.00	100.00	100.00

VITA

Korey Herrman

Candidate for the Degree of

Master of Science

Thesis: MECHANICAL AND RADIATION SHIELDING PROPERTIES OF BORON NITRIDE REINFORCED HIGH-DENSITY POLYETHYLENE

Major Field: Materials Science and Engineering

Biographical:

Education:

Master of Science (July 2020) in Materials Science and Engineering, Oklahoma State University, Tulsa, OK.

Bachelor of Science (May 2017) in Chemical Engineering, University of Arkansas, Fayetteville, AR.

Academic Employment:

Graduate Research Assistant, Department of Materials Science and Engineering, Oklahoma State University, Aug 2017 – July 2020.

Advanced Materials and Engineering Intern, NASA Langley Research Center, Hampton, Virginia. Jan 2018 – May 2018.

Academic Awards:

Materials Science and Engineering Outstanding Graduate Student, College of Engineering, Architecture & Technology, Oklahoma State University. April 2019.

Advanced Materials and Processing Branch Exceptional Contribution Award. NASA Langley Research Center, Hampton, Virginia. May 2018

Professional Membership:

Graduate and Professional Student Government Association – MSE Rep.
SAMPE – OSU Chapter President
HRC Graduate Student Organization and Material Research Society Member